



Forest Fire Damage Assessment and Biomass loss using Sentinel-2 Satellite Imagery
in Doi Inthanon National Park in Chiangmai Province, Thailand

CHATPONG SOMMAI

A THESIS SUBMITTED IN PARTIAL FULFILLMENT OF
THE REQUIREMENTS FOR MASTER OF SCIENCE
IN GEOINFORMATICS
FACULTY OF GEOINFORMATICS
BURAPHA UNIVERSITY

2020

COPYRIGHT OF BURAPHA UNIVERSITY

การประเมินพื้นที่เสียหายจากไฟป่าและความสูญเสียของมวลชีวภาพเหนือพื้นดินด้วยดาวเทียม
Sentinel-2 ณ อุทยานแห่งชาติดอยอินทนนท์ จังหวัดเชียงใหม่



นั้ตรพงศ์ สมหมาย

วิทยานิพนธ์นี้เป็นส่วนหนึ่งของการศึกษาตามหลักสูตรวิทยาศาสตรมหาบัณฑิต
สาขาวิชาภูมิสารสนเทศศาสตร์
คณะภูมิสารสนเทศศาสตร์ มหาวิทยาลัยบูรพา
2563
ลิขสิทธิ์เป็นของมหาวิทยาลัยบูรพา

Forest Fire Damage Assessment and Biomass loss using Sentinel-2 Satellite Imagery
in Doi Inthanon National Park in Chiangmai Province, Thailand



CHATPONG SOMMAI

A THESIS SUBMITTED IN PARTIAL FULFILLMENT OF
THE REQUIREMENTS FOR MASTER OF SCIENCE
IN GEOINFORMATICS
FACULTY OF GEOINFORMATICS
BURAPHA UNIVERSITY

2020

COPYRIGHT OF BURAPHA UNIVERSITY

The Thesis of Chatpong Sommai has been approved by the examining committee to be partial fulfillment of the requirements for the Master of Science in Geoinformatics of Burapha University

Advisory Committee

Examining Committee

Principal advisor

.....

(Professor Shao Zhengfeng)

..... Principal
examiner

(Professor Timo Balz)

..... Member
(Professor Lingli Zhao)

..... Member
(Dr. Tanita Suepa)

..... Member
(Dr. Haoran Zhang)

..... External
Member
(Professor Orhan Altan)

..... Dean of the Faculty of Geoinformatics
(Lecturer Dr. Kitsanai Charoenjit)

.....

This Thesis has been approved by Graduate School Burapha University to be partial fulfillment of the requirements for the Master of Science in Geoinformatics of Burapha University

..... Dean of Graduate School
(Associate Professor Dr. Nujjaree Chaimongkol)

.....

61910088: MAJOR: GEOINFORMATICS; M.Sc. (GEOINFORMATICS)

KEYWORDS: Sentinel-2, Burn index, Spectral indices, Burn area, Aboveground Biomass

CHATPONG SOMMAI : FOREST FIRE DAMAGE ASSESSMENT AND BIOMASS LOSS USING SENTINEL-2 SATELLITE IMAGERY IN DOI INTHANON NATIONAL PARK IN CHIANGMAI PROVINCE, THAILAND .
ADVISORY COMMITTEE: SHAO ZHENGFENG, 2020.

Forest fire is a significant disturbing factor in ecosystems that influence land cover alteration. Now, it is generally realized that the global forest is greatly affected by fire. This research is the application of geoinformatics and remote sensing techniques in the analysis of the forest fire damage area in the Doi Inthanon national park in Chiangmai Province. The Sentinel-2 Satellites were used to analyze the burned area and forest monitoring due to Sentinel-2 satellite image data has a medium and high spatial resolution and temporal resolution of five days. From Thailand forest fires report, it is found that Thailand has problems due to forest fires every year and the impacts are quite devastating, particularly in northern Thailand. Forest fires tends to increase over recent decades, with most of the increase in dry season beginning from January to May with its peak in March. According to the statistics of forest fires occurrences in Thailand in 2016-2019, it shows the results of more than 7 million rai or approximately 11,538.4272 square kilometers of burned areas (DNP, 2019; GISTDA, 2019). Therefore, the solution to solve this problem should be significantly taken into account. This study aims to detect forest fire burned scars and the classification of burn severity in Doi Inthanon National Park in 2019. We found that Forest fires in the studied area occurred during the period from January 1 to May 31, 2019 and the highest is in March. in the study area, we found 553 of active fire hotspots and most of these hotspots are in the area of deciduous forests, these hotspots have been conducted by the Fire Information for Resource Management System (FIRMS, 2019). The analysis of the damaged areas of forest fires were calculated using Differenced Normalized Burn Ratio (dNBR), Relativized Burn Ratio (RBR) and Burned Area Index for Sentinel-2(BAIS2) and compared with the burn area published by the Geo-informatics Technology Development Agency (GISTDA) of

Thailand. The result showed that RBR, BAIS2 and dNBR are good performance and consistent with the actual area of the forest fire. The overall accuracy of the detection of burned area of three indices were 90.00%, 87.14%, 81.43% (Kappa coefficient = 0.81, 0.75, 0.64), respectively.

Moreover, when considered the fire problems mentioned above, it can be said that forest is the area that is profoundly affected by the fire. Biomass and ecological systems were destroyed by fire. The loss of the biomass causes various impacts on forests and environment. Forests also play a major role in absorbing carbon dioxide (CO₂) throughout the process of photosynthesis. This stage produces organic substances; carbon-based components that are stored in various parts of the tree, known as Aboveground biomass. For this reason, the studies on evaluation of biomass and carbon storage are very important. Remote sensing has been applied in the field of forest surveys for decades and has become a quality method for estimating aboveground biomass (AGB) and carbon stocks of trees. Lately, Random Forest (RF) and Support Vector Machine (SVM) in machine-learning model were used to improve the accuracy of satellite image analysis with a more complex algorithm. In this section, the burned area of the RBR index is used to assess the loss of above-ground biomass, and the result found that most of the burned areas are the deciduous forests. This study aims to evaluate the ability of Sentinel-2 images using vegetation indices and AGB obtained from field measurements, to compare and evaluate the accuracy of the AGB prediction models and to create the map of AGB loss in the burned area by optimal models. The Vegetation indices (Vis) combine and forest inventory parameters were used to estimate above-ground biomass loss in damage area from forest fires and compare the accuracy of the biomass model using Machine Learning method (RF, SVM). 47 sample plots and 5 vegetation indices in dry dipterocarp forest and mixed deciduous forest area were considered to calculate the loss of aboveground biomass. Evaluate the efficiency of the model using The 6-fold cross-validation. The results show that the RF model is the lowest root mean square error (RMSE= 6.04 Mg/ha) from predicted and observed AGB (Ws+Wl+Wb) and highest coefficient of determination ($R^2 = 0.98$). The average predicted AGB was 108.815 Mg/ha. Mean absolute error (MAE) of RF was 4.17 Mg/ha. Consequently, The results show that the

RF model AGB of leaves ($R^2 = 0.93$, RMSE= 0.277 Mg/ha). The average predicted AGB loss of leaves was 2.91 Mg ha. Thus, the RF model was the most accurate model for estimating AGB in this study area. These results demonstrated that Sentinel-2 satellite is a source of valuable information for the monitor after the fire event. It is also suitable for assessing the changes in vegetation, forestry, agriculture and other areas. Furthermore, the application of satellite data with machine learning algorithms indicates the effective potential to assess aboveground biomass.



ACKNOWLEDGEMENTS

I would like to express my sincere thanks to my thesis supervisor, Professor Shao Zhenfeng for his expert advice invaluable and encouragement throughout the course of this research.

In addition, I am grateful for the teachers of SCGI Master Program; Dr. Kitsanai Charoenjit, Asst.Prof.Dr. Parin Lopittayakorn, Dr. Tanita Suepa, Dr. Haoran Zhang and Miss Ya Zhang from Wuhan University for their extraordinary support and help in this thesis process.

I would like to thank National park, Wildlife and Plants Department, Thailand for helping granting permission to study in the research area.

This research would have been impossible without the support of The Sirindhorn center of Geo-Informatics Master's Program which is a collaboration among Wuhan University: China, Burapha University: Thailand, Geo-informatics Technology Development Agency (GISTDA) under Ministry of Science and Technology, Thailand and Royal Forest Department, Thailand.

Finally, I would like to thank you very much to my family and friends for supporting and helping me throughout the period of this research.

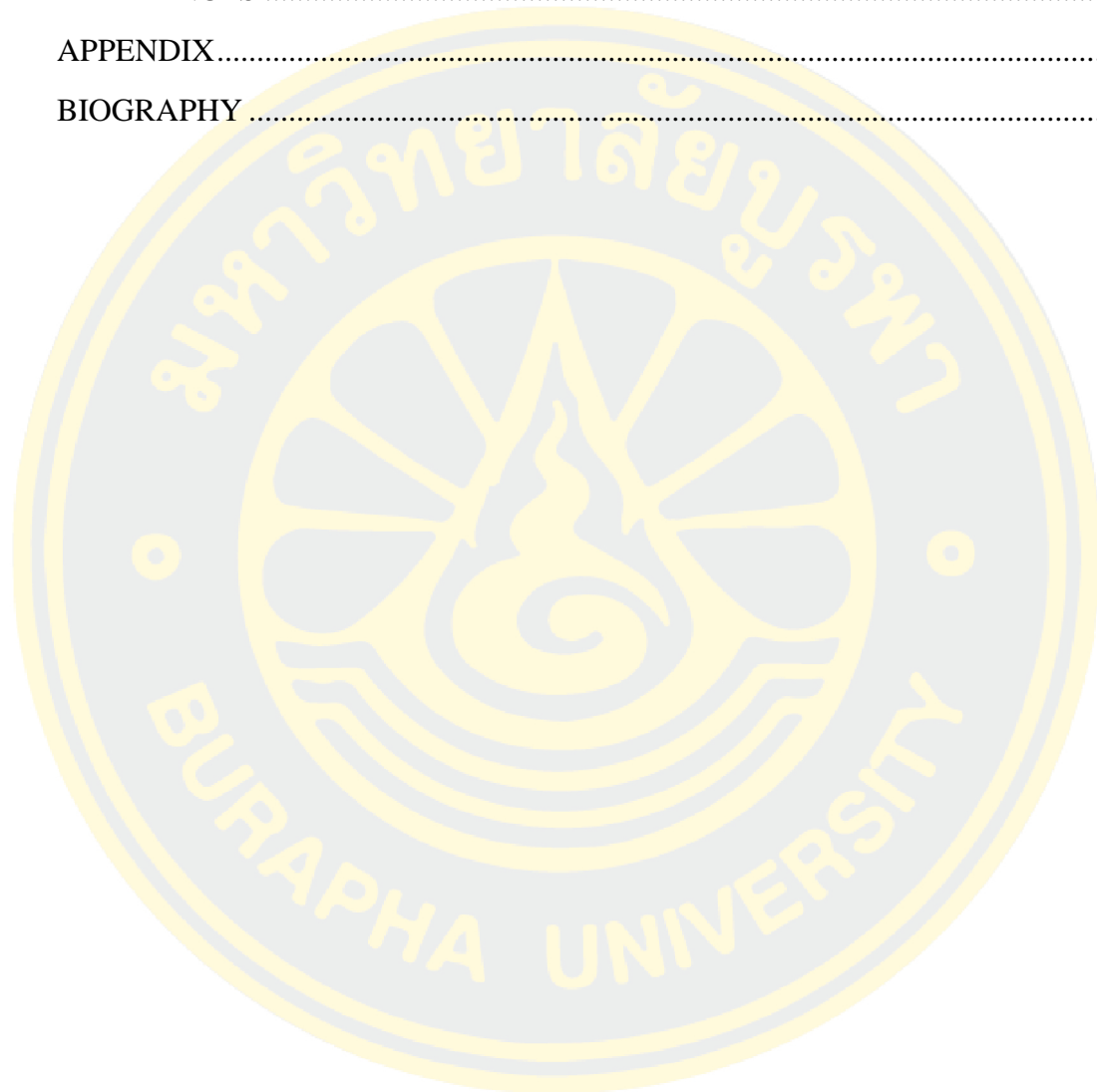
Chatpong Sommai

TABLE OF CONTENTS

	Page
ABSTRACT.....	D
ACKNOWLEDGEMENTS.....	G
TABLE OF CONTENTS.....	H
LIST OF TABLES.....	K
LIST OF FIGURES.....	L
1. INTRODUCTION.....	1
Statements and significance of the problems.....	1
Research Objectives.....	3
Research Question.....	3
Thesis Structure.....	3
2. LITERATURE REVIEW.....	5
Forest fires in Thailand and detection of fires.....	5
Active fire hotspot data from MODIS.....	5
Active Fires Hotspot from VIIRS product.....	6
The statistics of forest fire occurrences in Thailand, the year 2016-2019.....	7
Sentinel-2 Satellite images.....	9
Classification of burned areas and burn severity level using Sentinel-2 satellite.....	11
Burned areas indices.....	11
Burned severity level.....	12
Machine Learning.....	12
Supervised Learning.....	14
Unsupervised Learning.....	17
Biomass and Allometric Equation.....	17
Spectral indices from Sentinel-2 satellite.....	18

Related studies with Mapping of burned areas and burn severity and estimate biomass using Satellite image by Machine learning (ML) algorithms to predict biomass	19
3. RESEARCH METHODOLOGY	22
Study site	22
Materials	25
Instruments	25
Software.....	25
Methods	26
1. Pre-processing	27
2. Burn area classification	27
3. Burn Classification accuracy	28
4. Kappa coefficient	29
5. Field data collection	29
6. Spectral indices of Sentinel-2 satellite image.....	31
7. Modeling the Relationship between Field AGB and Satellite Data	31
8. Statistics analysis.....	32
4. EXPERIMENT RESULT AND DISCUSSION	33
Burn area classification.....	33
1. Differenced Normalized Burned Ratio (dNBR).....	33
2. Relativized Burn Ratio (RBR)	34
3. Burned Area Index for Sentinel-2 (BAIS2) Classification	37
4. Burned area published GISTDA (referenced data)	38
Burn Classification accuracy and Burn severity map.....	41
Above ground biomass estimation.....	45
1. Calculation of Vegetation Indices using Sentinel-2 satellite image.....	45
2. Calculation of AGB from field measurement	46
3. The Value of Vegetation indices in deciduous forest sample plot	47
4. Aboveground biomass modelling, Statistical analysis	49

5. Result of AGB mapping by Machine Learning regression model	51
Discussion.....	54
5. CONCLUSION AND FUTURE WORK.....	57
REFERENCES	59
APPENDIX.....	64
BIOGRAPHY	69



LIST OF TABLES

	Page
Table 1. MODIS in Thailand, the year 2017-2019 (1 January - 31 May)	5
Table 2. MODIS in the Northern region of Thailand, the year 2017-2019 (9 Province).....	5
Table 3. VIIRS product spatial resolution of 375 m in Thailand, the year 2018-2019	6
Table 4. VIIRS product in the northern region of Thailand, the year 2017-2019 (9 Province).....	7
Table 5. The statistics of forest fire occurrences in Thailand, the year 2016-2019.....	8
Table 6. The statistics of forest fire occurrences in Thailand, the year 2016-2019.....	8
Table 7. The statistics of forest fire occurrences in conservation area in the Northern region of Thailand.....	9
Table 8. Original bands.....	10
Table 9. Burn severity levels	12
Table 10. The spectral indices	18
Table 11. List of the material.....	25
Table 12. The List of Software	25
Table 13. Allometric Equation.....	30
Table 14. Classification of burned area and unburned (dNBR).....	33
Table 15. Classification of burned area and unburned (RBR).....	35
Table 16. Classification of burned area and unburned (BAIS2).....	37
Table 17. Classification of burned area and unburned (reference).....	39
Table 18. Accuracy assessment	41
Table 19. Descriptive of Above ground biomass estimation from field measurement...	46
Table 20. Value of Vis indices in plot.....	47
Table 21. Performance estimation of SVR and RF models.	50
Table 22. Performance estimation of SVR and RF models.	50
Table 23. Comparison of previous studies with machine learning.....	56

LIST OF FIGURES

	Page
Figure 1 Comparisons between Sentinel-2 and Landsat 7,8 sensor.....	10
Figure 2 The difference of the NIR and SWIR in burned and vegetation areas.....	11
Figure 3 Comparisons between Traditional Programming with Machine Learning	13
Figure 4 Type of Machine Learning	14
Figure 5 basic form of Supervised Learning.....	14
Figure 6 basic form of Random Forest Algorithm and Support vector machine.....	16
Figure 7 Study area	22
Figure 8 Forest type	23
Figure 9 Active Fire Hotspot	24
Figure 10 Flowchart of the research method	26
Figure 11 Pre-fire event on 26 December 2018 and Post-fire on 31 March 2019 image.....	28
Figure 12 Square sample plot and standard method to mea-sure the size of tree.....	30
Figure 13 dNBR classification map	33
Figure 14 dNBR classification map.....	34
Figure 15 RBR classification map	35
Figure 16 RBR classification map	36
Figure 17 BAIS2 classification map	37
Figure 18 BAIS2 classification map	38
Figure 19 Reference classification map.....	39
Figure 20 Map of the main forest types affected by fires and comparison of the number of active fire hotspots in burned class.....	40
Figure 21 Location of checkpoints in the study area	42
Figure 22 Burn severity map of RBR	43
Figure 23 Comparison of Burned map.....	44
Figure 24 Vegetation Indices (VIs) using Sentinel-2 optical satellite image	45

Figure 25 AGB predicted distribution in burned area52

Figure 26 AGB of leaves predicted distribution in burned area53



1. INTRODUCTION

Statements and significance of the problems

In the present time, one of the serious problems that have a broad impact on humans around the world is climate change. Global warming which refers to the rise in global temperatures is one aspect of climate change. The major cause of global warming is caused by human activities that are the sources of pressure on the environment. Those activities include the encroachment, deforestation, forest fires, burning fuel from coal, oil and natural gas, toxic fumes from various industrial, dust from mining and toxic fumes from automobile exhaust. These activities cause pollution which severely affect the ecosystems of living organisms both land and sea. Forest fire performs an important role in nutrient cycling and the structure of biodiversity and habitat. However, if it occurs uncontrollably, it may cause a serious damage to environment. Recently, Forest fires and smog situations have analyzed by the Geo-informatics Technology Development Agency (GISTDA) and National Park, Wildlife and plants Department of Thailand. They found that Thailand has problems due to forest fires every year and the impacts are quite devastating, particularly in northern Thailand. Forest fires tends to increase over recent decades, with most of the increase in dry season beginning from January to May with its peak in March. According to the statistics of forest fires occurrences in Thailand in 2016-2019, it shows the results of more than 7 million rai or approximately 11,538.4272 square kilometers of burned areas (DNP, 2019; GISTDA, 2019). Therefore, the solution to solve this problem should be significantly taken into account.

The apply of remote sensing method to assess the forest fire damage areas is widespread on a global scale, such as the use of Actives fires and Hotspot from a sensor like Advanced Very High-Resolution Radiometer (AVHRR) and Moderate Resolution Imaging Spectroradiometer (MODIS) (FIRMS, 2019). At present, many areas around the world have used high-resolution satellite imagery to monitor the fire. However, these data are limited to access. From the study of the damaged areas of forest fires in the past of Thailand, we found that Landsat satellite image is the main data to detect burned areas, land use change and environmental impact estimation. Currently, The

European Space Agency (ESA) launched the Sentinel-2 satellite (Malenovský et al., 2012). The Multispectral Instrument (MSI) sensor records information in red-edge band which has the ability to detect chlorophyll content (CURRAN, DUNGAN, & GHGLZ3, 1990). Both Sentinel-2 and Landsat satellite are free which can be downloaded data on the website. Nevertheless, the Landsat-8 satellite data has lower spatial resolution than the Sentinel-2 satellite and temporal resolution sixteen days and five days, respectively. Thus, to the rapidity and assess the area affected by the fire and to monitor the vegetation loss to be more accurate and reliable, this study uses medium- high-resolution Sentinel- 2 satellite images combine with active fires hotspot from Fire Information for Resource Management System (FIRMS) website and reference information of relevant government agencies which is the geoinformatics organization.

In general, Burn severity mapping in Thailand was created by the dNBR (differenced NBR) based on Landsat Satellite image which the Near-infrared and Shortwave infrared wavelength were applied to computed in Normalized burn ratio(NBR) (Key & Benson, 2006). This equation is the most appropriate for detection burn severity. Moreover, in 2014 a new index was developed for Landsat burn severity, also known as the relativized burn ratio (RBR) index which was tested in the western US and they strongly recommend that as a strong alternative for detect burned and categorizing burn severity (Parks, Dillon, & Miller, 2014). Recently, new Burned Area Index for Sentinel-2 (BAIS2) was developed for post-fire mapping in 2018 by using satellite images of spatial resolution of 20 m to detect burned areas (Filipponi, 2018). in this study, burned areas were extracted using Sentinel- 2 satellite images and compared the result of dNBR, RBR and BAIS2 index. Moreover, when considered the fire problems mentioned above, it can be said that forest is the area that is profoundly affected by the fire. Biomass and ecological systems were destroyed by fire. The loss of these biomass causes various impacts on forests and environment. Forests also play a major role in absorbing carbon dioxide (CO₂) throughout the process of photosynthesis. This stage produces organic substances; carbon-based components that are stored in various parts of the tree, known as Aboveground biomass. For this reason, the study an evaluation of biomass and carbon storage are very important.

Remote sensing has been applied in the field of forest surveys for decades and have become a quality method for estimating aboveground biomass (AGB) and carbon

stocks of trees. Lately, Random Forest (RF) and Support Vector Machine (SVM) in machine-learning model were used to improve the accuracy of satellite image analysis with a more complex algorithm. Therefore, Sentinel-2 satellite images were used to calculate the loss of aboveground biomass in the burning area of study area. It is also suitable for assessing the changes in vegetation, forestry, agriculture and other areas

Research Objectives

Main objectives

The main objective is to assess the forest fires damage area from Sentinel-2 satellite images and estimate above-ground biomass loss in damage area by Vegetation indices (Vis) combine with forest inventory parameters

Specific objectives

1. To detect forest fire burned scars and Burn severity classification in Doi Inthanon National Park Chiang Mai Province in 2019
2. To evaluate the ability of Sentinel-2 images using vegetation indices and AGB obtained from field measurements.
3. To compare and evaluate the accuracy of the AGB prediction models
4. To create map of AGB loss in the burned area by optimal models

Research Question

1. What is the estimated amount of damage forest fires area and fire severity level in 2019?
2. How is the aboveground biomass per hectare?
3. How is the aboveground biomass loss in damage forest fires area?
4. Which biomass prediction models are the best for estimate AGB in the study area?

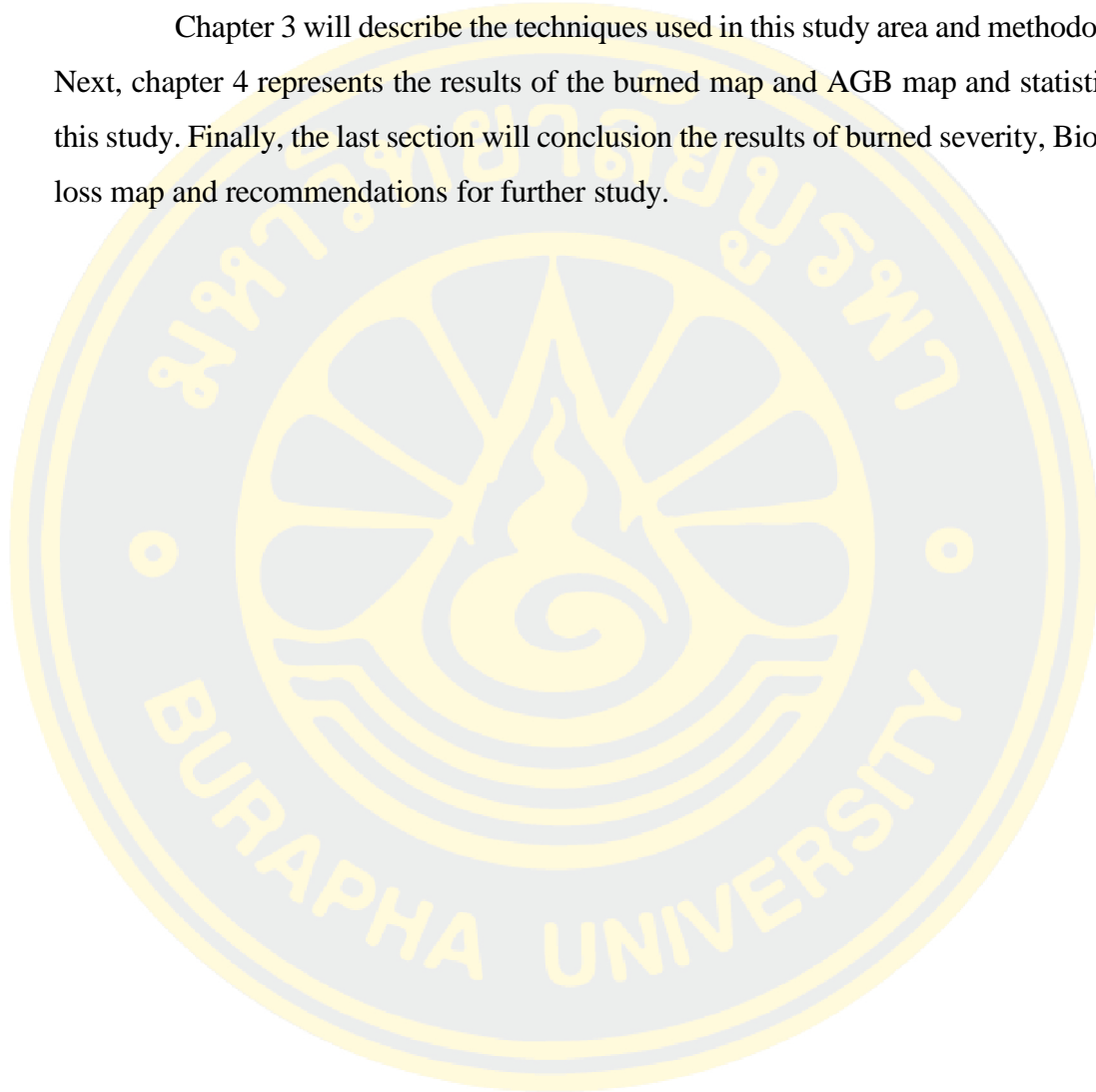
Thesis Structure

The structure is as follows:

Chapter 1 presented the statements and significance of the problems of forest fire and application remote sensing to monitoring and improve the accuracy of forest fire damage assessment using Sentinel 2 high resolution to estimation biomass loss, including

research problems and objectives of the study. Chapter 2 will provide an overview, Literature review topic about forest fires and detection of fires in Thailand and related studies with the mapping of burned areas and estimate biomass using Satellite image by Machine learning (ML) algorithms.

Chapter 3 will describe the techniques used in this study area and methodology. Next, chapter 4 represents the results of the burned map and AGB map and statistics in this study. Finally, the last section will conclusion the results of burned severity, Biomass loss map and recommendations for further study.



2. LITERATURE REVIEW

Forest fires in Thailand and detection of fires

The report “Summary of forest fires and smog situations with satellite images” (GISTDA, 2019) Active fire hotspot data from TERRA and AQUA satellites. The MODIS system continues to be used to monitor forest fires and smog situations that occur annually.

GISTDA conducted heat analysis combine with geo-informatization layers from relevant departments in 9 northern provinces in Thailand. Including reporting from the website <http://fire.gistda.or.th>. Consists of the following details:

Active fire hotspot data from MODIS

Table 1. MODIS in Thailand, the year 2017-2019 (1 January - 31 May)

Month	2017	2018	2019
January	1,737	2,167	4,407
February	4,968	3,878	7,245
March	6,930	5,098	10,810
April	2,006	3,143	5,283
May	365	279	1,506
Total	16,006	14,565	29,251

Table 2. MODIS in the Northern region of Thailand, the year 2017-2019
(9 Province)

Province	2017	2018	2019
Chiang Rai	210	226	1,951
Chiang Mai	904	650	1,723
Nan	597	546	1,340
Phayao	115	86	541
Phrae	310	235	690

Province	2017	2018	2019
Mae Hong Son	1,188	915	1,633
Lampang	663	429	1,067
Lamphun	333	258	326
Tak	1,098	1,377	946
Total	5,418	4,722	10,217

Unit rai = multiply * 1,600 squaremeters

Active Fires Hotspot from VIIRS product

The measurement of the accumulated heat points with the VIIRS installed on the Suomi NPP (National Polar-orbiting Partnership) satellite. Especially, the accumulation of heat of TERRA / AQUA satellite in the MODIS system has been in use for over 15 years. VIIRS is a system installed on satellites with similar MODIS orbits. But there is a difference in the spatial resolution.

The VIIRS system detects the accumulated heat spots from the data layers with details of 375 meters and 750 meters per pixel. As a result, the number of heat points collected from this system and accumulating approximately three times more than the MODIS system due to its ability to detect small heat points or low heat point.

The improved resolution will be useful for observing and collecting data, including the ability to create a model and forecast changes in the behavior of the fire and helpful for forest fire management decisions.

According to Suomi NPP satellite data, the VIIRS system has found the most accumulated heat spots in Thailand in 2019 of 205,373 points, with the highest accumulation of 73,936 points in conserved forests in 2019.

Table 3. VIIRS product spatial resolution of 375 m in Thailand, the year 2018-2019

Month	Active Fires Hotspot 2018	Active Fires Hotspot 2019
January	9,873	19,837
February	21,902	47,558
March	41,315	80,307

Month	Active Fires Hotspot 2018	Active Fires Hotspot 2019
April	23,632	45,223
May	12,448	12,448
Total	109,170	205,373

Unit rai = multiply * 1,600 squaremeters

Table 4. VIIRS product in the northern region of Thailand, the year 2017-2019
(9 Province)

Province	2017	2018	2019
Chiang Rai	1,233	1,214	10,847
Chiang Mai	7,607	6,496	16,875
Nan	3,590	2,848	8,790
Phrae	3,061	1,870	7,162
Mae Hong Son	9,703	8,524	16,320
Lampang	6,699	4,832	11,716
Lamphun	3,077	2,321	3,358
Tak	10,028	11,154	10,218
Payao	1,419	594	5,170
Total	46,417	39,853	90,456

Unit rai = multiply * 1,600 squaremeters

The statistics of forest fire occurrences in Thailand, the year 2016-2019

The analysis of burn areas from the Landsat-8 satellite image between 1st January-31st May showed that the burn areas increased.

Table 5. The statistics of forest fire occurrences in Thailand, the year 2016-2019

Province	Burn Scar(rai)		
	2,017	2018	2019
Chiang Rai	116,271	127,692	334,671
Chiang Mai	810,733	903,978	953,135
Nan	556,097	287,395	628,445
Phrae	358,866	189,845	404,430
Mae Hong Son	2,109,828	1,952,122	1,528,375
Lampang	1,361,044	565,140	1,022,112
Lamphun	561,384	176,924	502,949
Tak	1,728,624	1,227,614	1,550,228
Payao	268,669	94,533	287,172
Total	7,871,516	5,525,243	7,211,517

Source: (GISTDA, 2019)

Unit rai = multiply * 1,600 squaremeters

Table 6. The statistics of forest fire occurrences in Thailand, the year 2016-2019

Region	2016		2017		2018	
	Number of fires	Damaged area	Number of fires	Damaged area	Number of fires	Damaged area
Northern	4,550	70,602.4	3,492	60,774.3	2,685	43,437.0
North-East	1,560	26,709.3	873	10,647.7	879	9,699.1
Center and East	532	11,082.1	265	3,368.0	167	1,632.0
Southern	204	17,502.2	20	629.0	37	998.2
Total	6,846	125,896.0	4,650	75,419.0	3,768	55,766.3

Source: : (DNP, 2019)

Unit rai = multiply * 1,600 squaremeters

Table 7. The statistics of forest fire occurrences in conservation area in the Northern region of Thailand

Region	2017		2018		2019	
	Number of fires	Damaged area	Number of fires	Damaged area	Number of fires	Damaged area
Chiang Mai	1,408	22,055.2	1,223	15,055.1	2,536	36,744.9
Mae Hong Son	298	3,703.0	367	3,730.1	500	7,711.8
Lampang	374	5,686.0	232	4,303.0	361	6,585.0
Lamphun	278	6,398.0	243	5,995.0	368	13,070.0
Chiang Rai	86	831.8	43	281.6	347	7,775.9
Phayao	59	802.0	30	250.0	203	3,241.0
Phrae	78	726.0	54	525.0	135	2,449.0
Nan	127	2,240.3	69	1,133.7	230	3,877.0
Uttaradit	46	485.0	39	403.0	57	607.3
Total	2,754	42,927	2,300	31,677	4,737	82,062

Source: : (DNP, 2019)

Unit rai = multiply * 1,600 squaremeters

Sentinel-2 Satellite images

Sentinel-2 was developed and designed is by the European Space Agency (ESA) that consists of two multispectral satellites. Sentinel-2A and 2B. It was launched on 23rd June 2015 and 07th March 2017 respectively, the satellites are equipped with Multispectral Instruments (MSI). Sentinel-2 images has a moderate spatial resolution, which makes it suitable for a variety of purposes, such as vegetation monitoring, soil and water cover, and observation of waterways. Data are acquired on 13 spectral bands (ESA, 2015). Sentinel-2 data is available for download with or without atmospheric correction as a Level 2A or 1C product, respectively. Level 1C products have gone through geometric and radiometric corrections, along with ortho-rectification, whereas 2A products have undergone additional

atmospheric correction (ESA, 2015), Figure 1 shows the comparison between Sentinel-2 and Landsat 7,8 sensor

Table 8. Original bands

Bands	Name	Wavelength(nm)	Spatial resolution(m)
1	Coastal aerosol	443	60
2	Blue	490	10
3	Green	560	10
4	Red	665	10
5	Red-edge1	705	20
6	Red-edge2	740	20
7	Red-edge3	783	20
8	Near-infrared (NIR)	842	10
8A	Vegetation Red-edge	865	20
9	Water vapor	945	60
10	SWIR cirrus	1375	60
11	Shortwave Infrared1	1610	20
12	Shortwave Infrared2	2190	20

Source: (ESA, 2015)

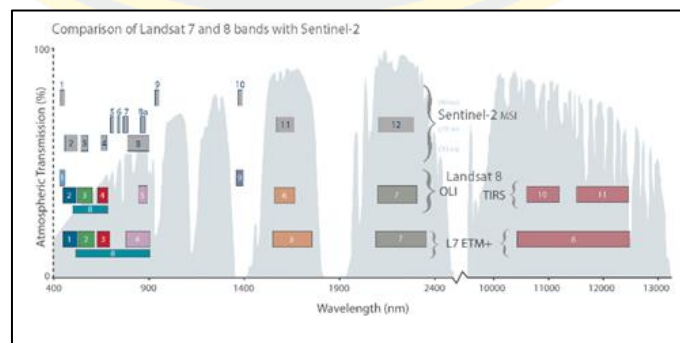


Figure 1 Comparisons between Sentinel-2 and Landsat 7,8 sensor

Source: (EROS, 2019)

Classification of burned areas and burn severity level using Sentinel-2 satellite

Burned areas indices

The Normalized Burn Ratio (NBR) is an index that is generated to focus on the burned area, which forms the equations that are similar to index NDVI. This equation uses the short-wave infrared red band instead of red band in NDVI. (Escuin, Navarro, & Fernández, 2008). Shortwave infrared band will represent high reflectance in burn area while the near infrared will represent low reflectance. In healthy vegetation, the near-infrared will represent high reflectance while shortwave infrared band will represent low reflectance. The values of unburned areas are usually attributed close to zero (Figure 2). The delta Normalized Burn Ratio (dNBR) was used to analyze the differences between before-fire and after-fire NBR and to analyze lately burned areas and differentiate them from bare land and other non-vegetated areas. However, the dNBR is able to detect the problems in areas with low before-fire vegetation cover, while NBR will perform less value in the change between before-fire and after-fire. In such cases, the relativized version of burn severity is more suitable to apply with those cases. So, Relativized Burn Ratio (RBR) will be used in this study.

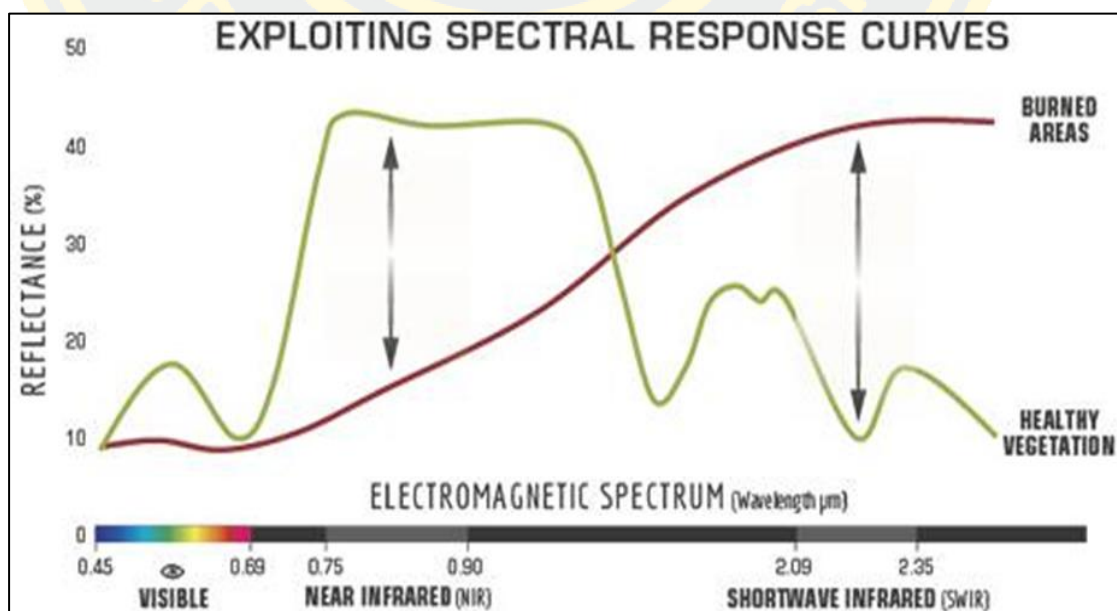


Figure 2 The difference of the NIR and SWIR in burned and vegetation areas

The Burned Area Index for Sentinel-2 (BAIS2) and dBAIS2 were developed by Filipponi (Filipponi, 2018) for burned area analysis. This equation was newly developed for the Sentinel-2 satellite image to assess the burning area using images before and after the fire occurred at 20 meters spatial resolution. It was designed to perform mapping and tested in many areas in Italy in 2017. The result showed an excellent performance to detect burning area. BAIS2 index is shown in the Table 10.

Water bodies can show similar NBR difference in certain circumstances, therefore, it is necessary to mask them out. For this purpose, we will create a single combined water and cloud mask. The Normalized Difference Water Index (NDWI) was used, to highlight the water body pixels (McFeeters, 2007)

Burned severity level

Burn severity levels based on the dNBR value were proposed by The United States Geological Survey (USGS), divided into 7 levels shown in the Table 9.

Table 9. Burn severity levels

Level	dNBR range (not scaled)
Enhanced Regrowth, High	-0.500 to -0.25
Enhanced Regrowth, Low	-0.250 to -0.101
Unburned	-0.100 to +0.099
Low Severity	+0.100 to +0.269
Moderate-Low Severity	+0.270 to +0.439
Moderate- High Severity	+0.440 to +0.659
High Severity	+0.660 to +1.300

Machine Learning

Machine Learning is a way for computers to learn and remember decision-making methods. It helps solve repeated problems that occur and there are no fixed rules for making decisions for machine Learning. Clear examples of machine learning systems include unmanned vehicle systems, automatic loan approval decision system, automatic loan approval decision system, translation system and the simulation system in being an expert in various sciences. (Bishop, 2006; Kohavi & Provost, 1998)

It can be seen that Machine Learning is used in almost everything that mimics the way people think and make decisions. So that computers can make their own decisions based on all-round information and get the right results, just as people make decisions. Thus, the machine learning system developers can build the system by doing two basic steps which are :

The first step is learning, which will bring the old data to practice (Training) with the computer for the computer to learn and remember the pattern. The result of the first step is the model used to predict or making decisions. After that, The second step will be predicted by the moment the event occurs entering data into the system.

The computer uses models that are already recognized from learning and it applies to real-time data and decides to take action. Therefore, the results will show that the user knows that the system can perform certain tasks similar to the person. (Figure 3)

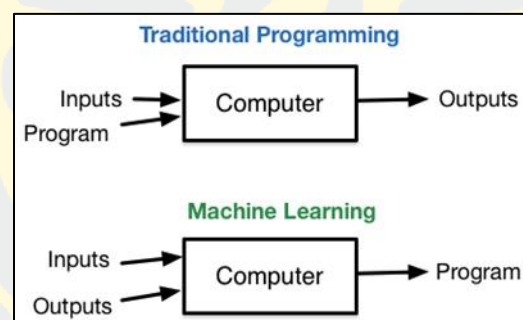


Figure 3 Comparisons between Traditional Programming with Machine Learning

Type of Machine Learning

All the algorithms in Machine Learning aim to create a mathematic model from the sample data. Therefore, we find that the most frequently used models are from statistics and probability because Machine Learning is the science of historical data retrieval and systematic data analysis in order to be able to predict the future. Since it is the science of historical data retrieval and systematic data analysis, it is able to predict the future. (Oladipupo, 2010)

In the figure below, the algorithm can be divided into two major categories: Supervised and Unsupervised (Figure 4), which means

Supervised Learning

Supervised Learning is a group of algorithms that focuses on teaching computers by studying the sample data to enable the computer to find the answer to the problem (solving) by itself, after learning from the sample data set that has been entered for some time.(Figure 5). Supervised Learning principles can be applied to solve problems in two type: Statistical Regression and Classification

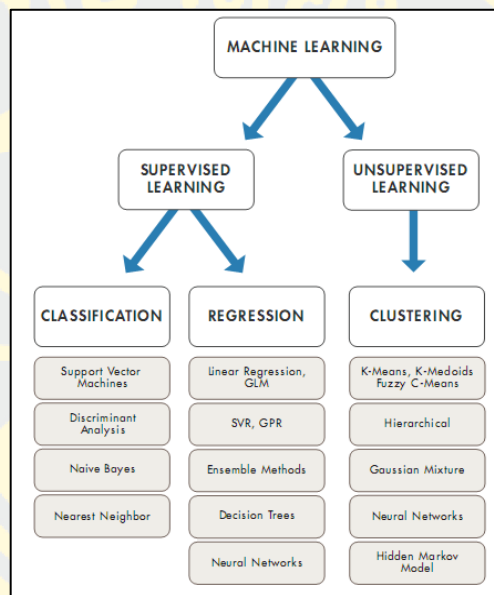


Figure 4 Type of Machine Learning

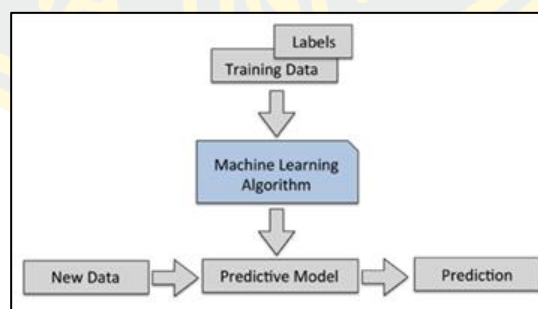


Figure 5 basic form of Supervised Learning

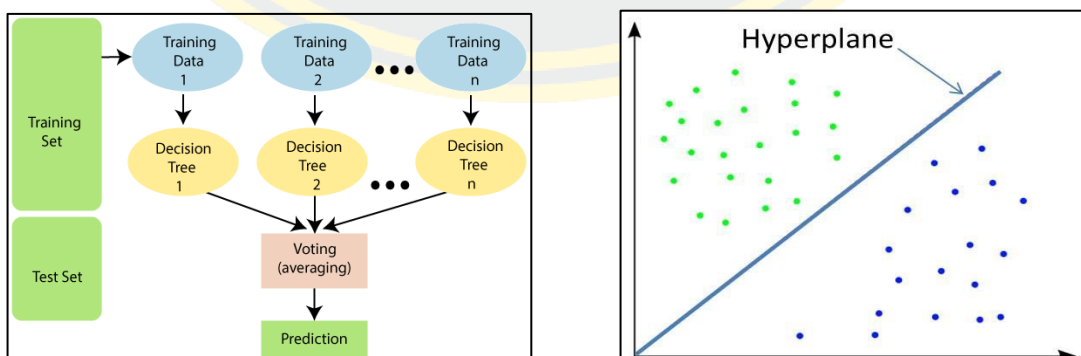
The figure above is the basic form of Supervised Learning. Labels are the part that determines the correct answer. The predictive model is the result of a practice or

model used to predict results. New Data is information that the computer does not recognize and prediction is the result that the computer predicted.(Alpaydin, 2014). In this study, focused on Random Forest Regression Model and Support vector Machine learning

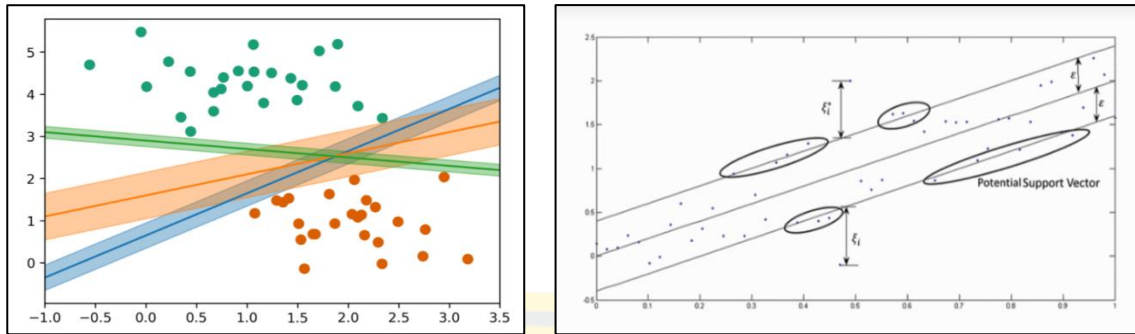
1. Random Forest Algorithm

Random Forest is a popular machine learning algorithm that belongs to the supervised learning technique. Classification and Regression problems can be done by using Random Forest Algorithm which is in machine learning. It depends on the concept of ensemble learning, which is a process of combining multiple classifiers to solve a complex problem and to improve the performance of the model. As the name suggests, "Random Forest is a classifier that contains a number of decision trees on various subsets of the given dataset and takes the average to improve the predictive accuracy of that dataset." Instead of relying on one decision tree, the random forest takes the prediction from each tree and based on the majority votes of predictions, and it predicts the final output.

The greater number of trees in the forest leads to higher accuracy and prevents the problem of overfitting. **Random Forest Regression:** The basic concept behind Random Forest is that it combines multiple decision trees to determine the final output. That is it builds multiple decision trees and merge their predictions together to get a more accurate and stable prediction, Figure 6 (a) below diagram explains the working of the Random Forest algorithm



(a) The basic concept of Random Forest (b) Hyperplane in Support Vector Machines



(c) The basic concept of Support Vector Machine

(d) Support Vector

Figure 6 basic form of Random Forest Algorithm and Support vector machine

2. Support Vector Machine

It is one of the machine learning models that is used to classify or segment data by creating a linear line that is used to divide the data (Hyperplane) and find the best line. (Figure 6 (b))

3. Max-Margin and Support Vectors

The data in the Support Vector Machines can be divided into many lines, the selected line will have the most margin, so the line with the widest range is the orange line with the most distance, resulting in less overfit or so-called soft Margin.

4. Kernels

Assuming that data in the study cannot be divided by linear, a non-linear of the Kernels method can be used to solve the problems.

The method is to create a dimension from 2D to 3D and then draw a line through the middle so that data can be divided into groups.

5. Support Vector Machine - Regression (SVR)

The Support Vector Regression (SVR) uses the same principles as the SVM for classification, with only a few minor differences.

First of all, because output is a real number it becomes very difficult to predict the information at hand, which has infinite possibilities. In the case of regression, a margin of tolerance (epsilon) is set in approximation to the SVM which would have already requested from the problem.

But besides this fact, there is also a more complicated reason, the algorithm is more complicated therefore to be taken in consideration.

However, the main idea is always the same : to minimize error, individualizing the hyperplane which maximizes the margin, keeping in mind that part of the error is tolerated (Padmapriya, 2015). (Figure 6 (c and d))

Unsupervised Learning

Unsupervised learning is in contrast to supervised learning. This type of learning does not specify the desired target variable. By having the computer process the relationship from the data itself.

Therefore, it can be said that this type of learning is non-teacher learning. (Xiao, 2015) (Bishop, 2006) Modeling using only input data without a target. There are 2 main uses: - Dimensionality reduction to reduce complexity before applying to display the results in graphs that can be read

Clustering of data according to features such as grouping customers according to their purchasing behavior.

Biomass and Allometric Equation

The above biomass (living above-ground biomass) is all parts of the tree that is above the ground, including the tree, branch, leaf, flower and fruit, as well as other plants. (TGO, 2011) or All living biomass above the soil, including stem, stump, branches, bark, seeds and foliage. (IPCC, 2006)

Allometric equation

An allometric equation is a technique of finding quantitative relationships between measurable characteristics of a tree.

For example, trunk diameter at breast height or height, and relate this to features that are more difficult to measure, like, for instance, the AGB. These relationships are usually both species and area-specific (Muukkonen, 2007)

Spectral indices from Sentinel-2 satellite

Table 10. The spectral indices

Spectral indices	Sentinel-2 Used formula	Equation	Reference
Normalized Burn Ratio (NBR)	$\frac{B8-B12}{B8+B12}$	(1)	(Key & Benson, 2006)
Difference Normalized Burn Ratio (dNBR)	PrefireNBR-PostfireNBR	(2)	
Relativized Burn Ratio (RBR)	$\frac{\text{PrefireNBR} - \text{PostfireNBR}}{\text{PrefireNBR}+1.001}$	(3)	(Parks et al., 2014)
Burned area index for Sentinel-2 (BAIS2)	$(1 - \sqrt{\frac{B6 \times B7 \times B8A}{B4}}) \times ((\frac{B12-B8A}{\sqrt{B12+B8A}} + 1))$	(4)	(Filipponi, 2018)
Normalized Difference Water Index (NDWI)	$\frac{B3-B8}{B3+B8}$	(5)	(McFeeters, 2007)
Normalized Difference vegetation Index (NDVI)	$\frac{B8-B4}{B8+B4}$	(6)	(Rouse, Jr., Haas, Schell, & Deering, 1974)
Normalized Difference vegetation Index Red-edge2 (RENDVI)	$\frac{B8-B6}{B8+B6}$	(7)	(J.-C. Chen et al., 2007)
Red-edge2 Ratio Vegetation Index (RERVI)	$\frac{B8}{B6}$	(8)	(Q. Cao et al., 2016)
Green Normalized Difference Vegetation Index (GNDVI)	$\frac{B8-B3}{B8+B3}$	(9)	(Gitelson, Kaufman, & Merzlyak, 1996)
Normalized Difference Vegetation Index (NDI45)	$\frac{B5 - B4}{B5 + B4}$	(10)	(Delegido, Verrelst, Alonso, & Moreno, 2011)

Related studies with Mapping of burned areas and burn severity and estimate biomass using Satellite image by Machine learning (ML) algorithms to predict biomass

Suresh Babu, Roy, and Aggarwal (2018) studied mapping of wildfires by using images of Sentinel in Pauri and Tehri Garhwal District in Uttarakhand. The RBR and dNBR indices were used to detect burned area and after that, it was compared to the active fire Hotspot. They found that both indices were able to detect forest fires which were excellent. In addition, the properties of the Sentinel satellites are several wavelengths, especially in the red wavelengths, in which the Red-edge band can analyze areas that contain chlorophyll.

According to Navarro et al. (2017) estimates the area of forest fires on Madeira Island using the image Sentinel 2A. They studied forest fire area using spectral indices of Sentinel 2 satellite images for instance, GNDVI, NDVI, NBR and Normalized difference Vegetation Index of red-edge spectral bands. The result demonstrated that NDVI-red edge indices presented better discretization of the burn levels than another index and Marino, Guillen-Climent, Ranz Vega, and Tomé (2016) found that the result indicated that the Difference Burn Area Index for MODIS (dBAIM) indices and Relativized Normalized Burn Ratio (RdNBR) indices had the best performance compared with reference data in Garajonay National Park by comparison between four spectral index.

Moreover, Filipponi (2019) The BAIS2 index were developed based on the Sentinel image. They found that the BAIS2 index for burned mapping was designed to be used with the Sentinel 2 characteristics. Comparative results between Copernicus EMS products and the NBR index represent the excellent performance of BAIS2 for detecting burned areas.

Mallinis, Mitsopoulos, and Chrysafi (2017) Studied and compared between Sentinel 2A Satellite and Landsat 8 Spectrum Index for assessing fire severity in Greece's Mediterranean pine ecosystem. Their studies show that the dNBR index of Sentinel 2A provides the highest correlation with ground estimates and it demonstrates the potential for assessing and mapping the severity of fire in the ecosystem.

Therefore, it can be seen that Sentinel-2 satellites has the potential to assess burning areas as many researchers have claimed in their studies for its effectiveness and high accuracy in the use of Sentinel-2 satellites.

In this research, the study related to the evaluation of above-ground biomass which many researchers have already studied about the assessment of biomass with remote sensing data. According to Askar, Nuthammachot, Phairuang, Wicaksono, and Sayektiningsih (2018), who evaluated the aboveground biomass by using vegetation indices from Sentinel-2 in evaluating the aboveground biomass (AGB) of private forests, forty five sample plots and seven vegetation indices were used to assess the ability of Sentinel-2 image in private forest. The comparison of vegetation indices and AGB value represents that the NDI45 index shows a higher correlation than other indices ($R^2 = 0.79$, $r = 0.89$).

From the study of Askar et al., 2018, The AGB values in this study are higher than the AGB values from other forest types. This is an indicator that the private forest is a forest with high biomass storage. In addition, vegetation indices from Sentinel 2 satellites image can provide good results in the AGB value on private forest.

At present, new algorithms have been developed for the analysis of biomass. Many researchers attempt to study and experiment or compare various models including developed the equation to calculate above-ground biomass and carbon stock. These researchers have shown the results that machine learning algorithms are useful for predicting biomass. In the study of L. Chen, Ren, Zhang, Wang, and Xi (2018),

They have developed predictions of biomass using four models: geographically weighted regression model, the artificial neural network, random forest regression, support vector machine regression. The results show that SVR (RMSE = $0.08 \text{ Mg} \cdot \text{ha}^{-1}$, $R^2 = 1$, AGB ranged from 17.32 to $316.92 \text{ Mg} \cdot \text{ha}^{-1}$) was the optimal model for AGB predictions in Changbai Mountains, Jilin Province, China. Eighteen vegetate indices from Sentinel- 2 satellite were used to analyze the relationship between above ground biomass and four model.

When compared with the previous study of Luodan Cao (L. Cao, Pan, Li, Li, & Li, 2018) by combining optical data and LIDAR data in the Heihe River Basin in China, they used four vegetation indices and Five method Random Forest (RF), Support Vector Machines (SVM), Back Propagational Neural Networks (BPNN), K-Nearest Neighbor (KNN), Generalized Linear Mixed Model (GLMM) for estimating forest AGB, The results show that the RF was the best model and The most suitable model is the RF model, which is the combination of LiDAR data and Optical (RMSE = 13.352 t/ha).

Moreover, Wu et al. (2016) also found that the RF algorithm (RMSE = 26.4 Mg_{ha}⁻¹) showed higher results than the SVR model in predicting biomass and the average biomass 89.43 tons/ha. From the research, it indicates that machine-learning approaches are effective and suitable for assessing biomass in Zhejiang Province, China.



3. RESEARCH METHODOLOGY

Study site

Doi Inthanon National Park was declared as a national park in 1972, which is the 6th national park in Thailand with an area of approximately 466 square kilometers (Latitude 18.542332 N, longitude 98.550403 E). It covers the area in Chom Thong district, Mae Chaem District, Mae Wang District and Doi Lo sub-district Chiang Mai Province (Figure 7).

In terms of topography, the topography consists of complex mountains and an elevation of 400-2,565 meters above mean sea level and Doi Inthanon is the highest peak in Thailand.

The main forest type is hill evergreen forest in the northern part and dry dipterocarp forest in the southern part of the area. Forest and land fires mostly occur in lowland areas or deciduous forest area (Figure 8).

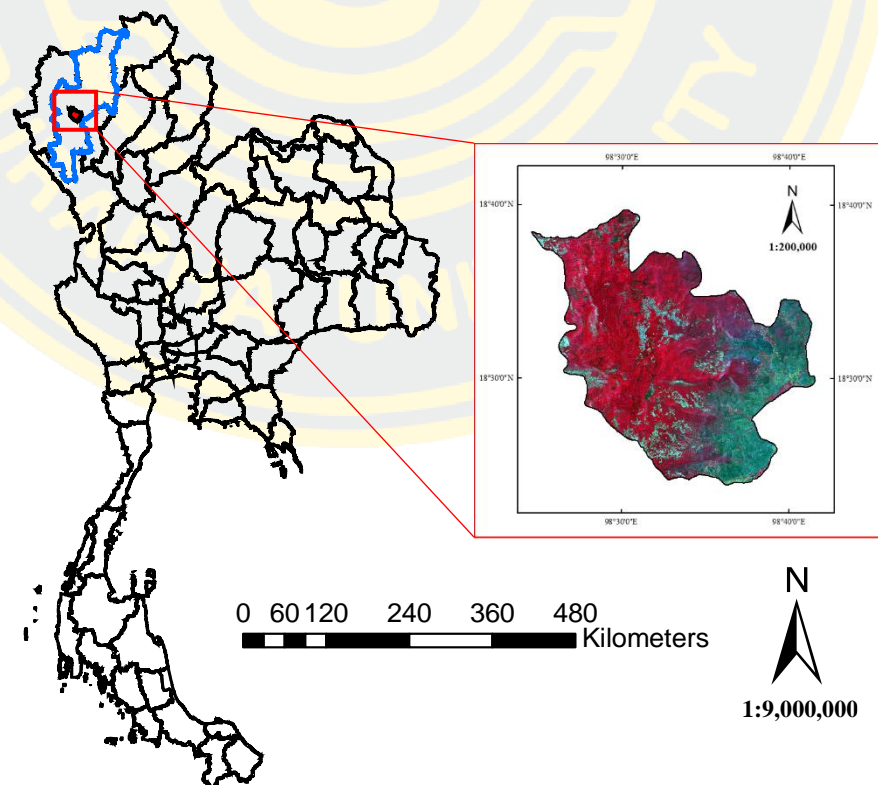


Figure 7 Study area

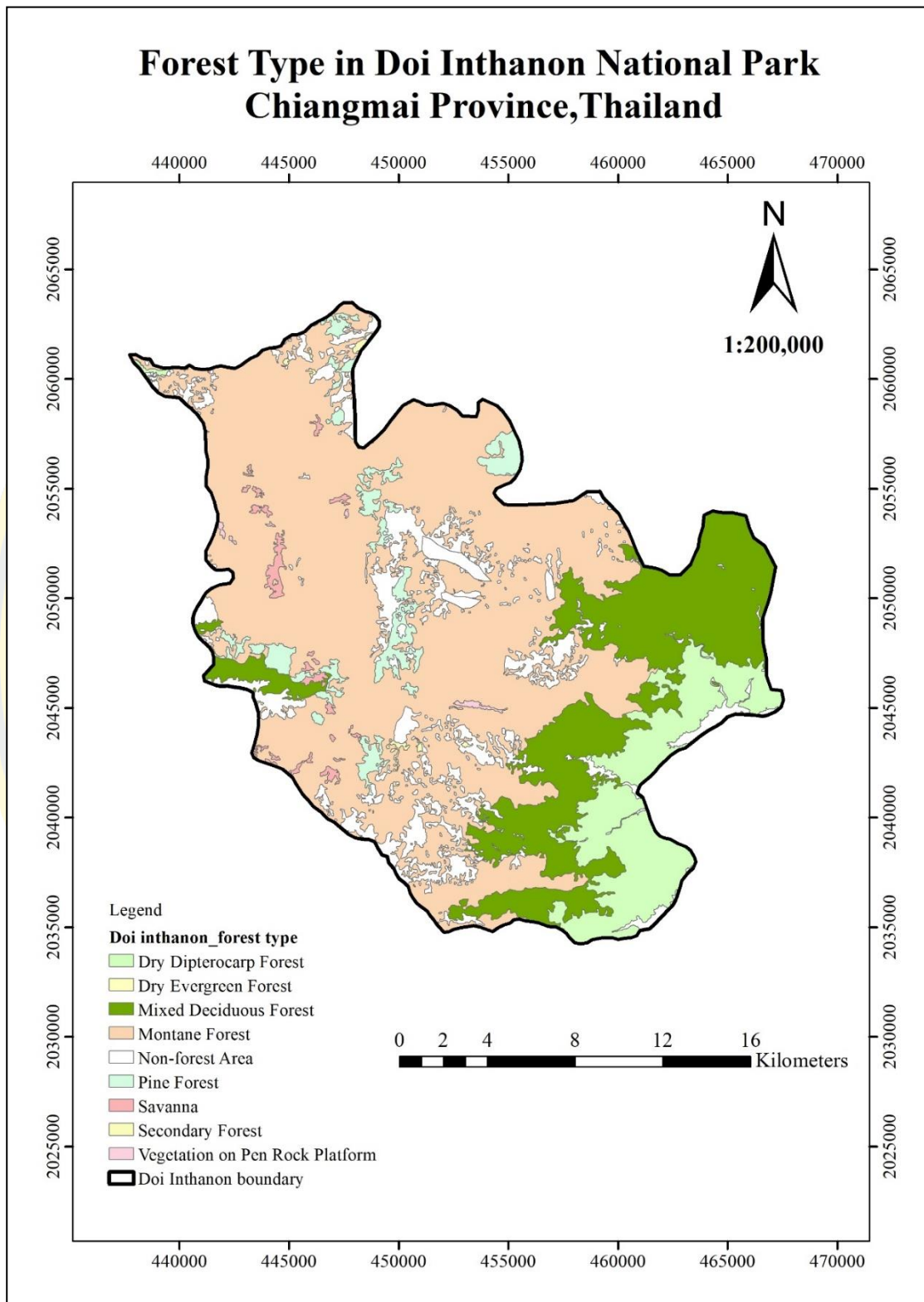


Figure 8 Forest type

Tree species

The number of trees found was 140 specific species in study area. Such as *Shorea obtusa* Wall., *Shorea siamensis* Miq., *Terminalia alata* Heyne ex Roth, *Adenanthera pavonina* Linn., *Dalbergia oliveri* Gamble ex Prain, *Gardenia sootepensis* Hutch., *Memecylon scutellatum* Naud., *Xylia xylocarpa* (Roxb.) Jaub. Var. *Kerri*. Craib & Hutch.) Nielsen, *Stereospermum neuranthum* Kurz, *Bombax vaeletonii* Hichr, *Dalbergia oliveri* Gamble ex Prain, *Dipterocarpus tuberculatus* Roxb (DNP, 2007)

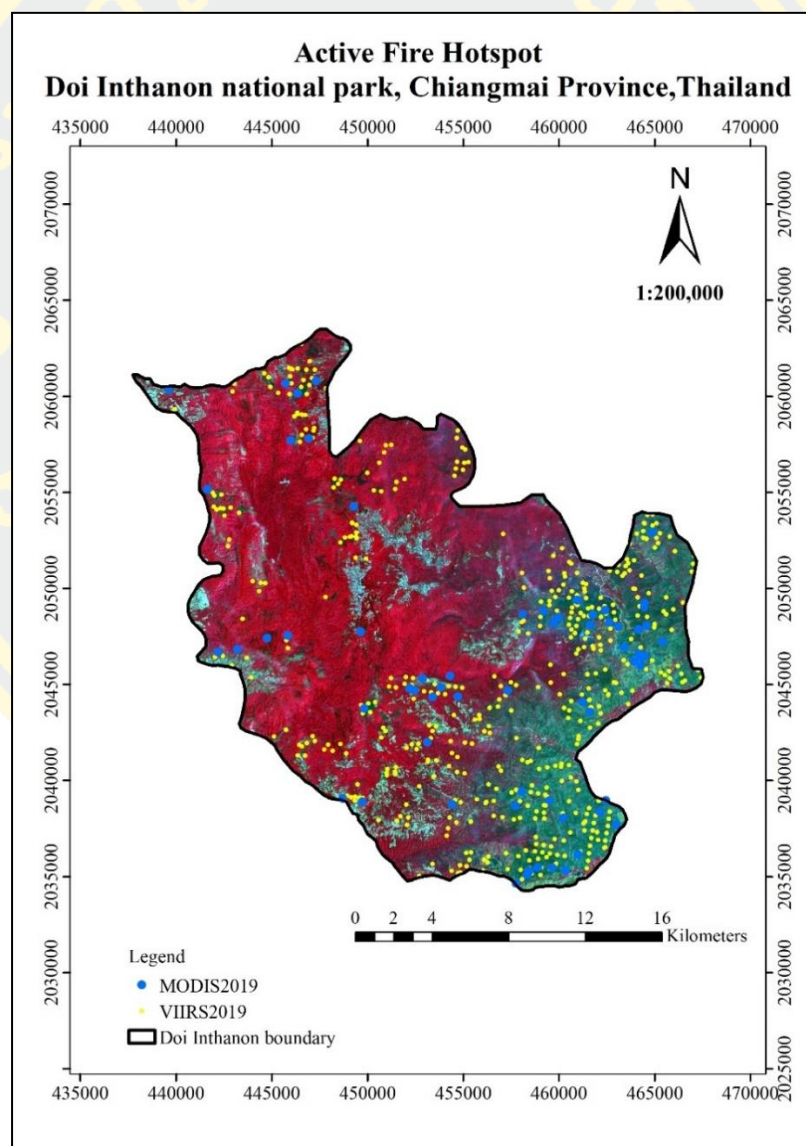


Figure 9 Active Fire Hotspot

Source: (RFD, 2018)

Materials

Instruments

Table 11. List of the material

Materials	Objectives
Measuring Tape (30m) Diameter tape (5m) Vertex hypsometer Garmin GPS	To outline plot DBH measurement Tree Height measurement Navigation and Mark location
Sentinel-2 image -Sentinel 2B data on 26 December 2018 -Sentinel 2A data on 31 March 2019 in Dry season or summer season download from the Copernicus Data Hub (ESA)	Spectral indices
MODIS data and VIIRS data shown in Figure 9	Detect heat sources/ accuracy assessment
Burned area data from GISTDA Based on Landsat 8 imagery	For Validation/accuracy assessment
Conservation boundary /Forest Type GIS data From DNP and Royal Forest Department (RFD)	For classification forest area

Software

Table 12. The List of Software

Software	Purpose
SNAP Toolbox ENVI, ArcGIS and QGIS Spyder python Microsoft office	Resampling sentinel and image processing Image processing Test model Statistical analysis and report

Methods

The method of study is divided into two main steps. (Depending on the purpose of the study)

Step 1: This step involves using Sentinel-2 satellite to assess the damaged areas from forest fires and burn severity classification

Step 2: Vegetation indices of the Sentinel-2 satellites are used to evaluate the AGB combine with the AGB calculation using the Allometric equation and compare the accuracy of the biomass model using Machine Learning method (Figure 10)

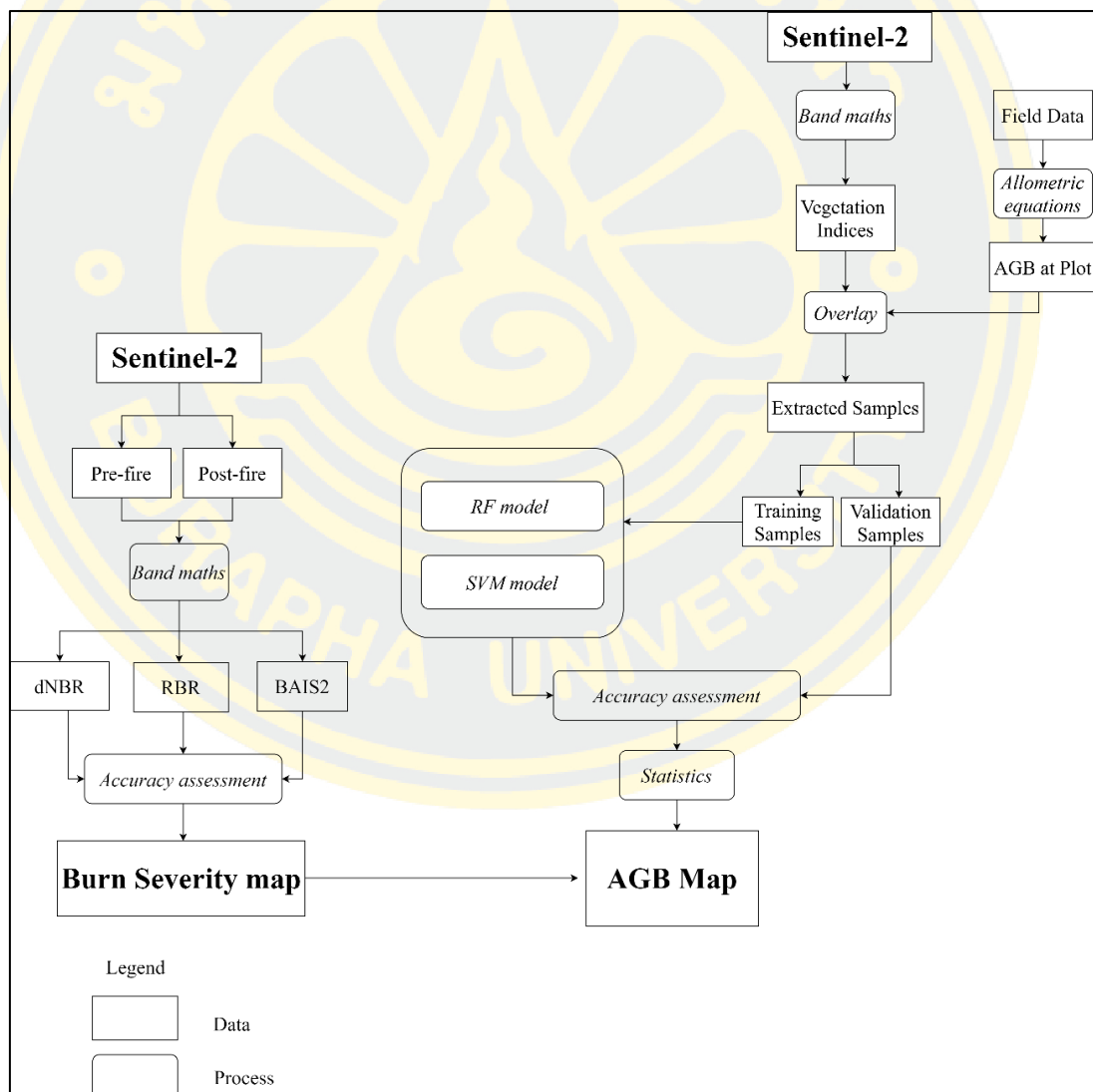


Figure 10 Flowchart of the research method

1. Pre-processing

Sentinel-2 images (MSI Level-2A) were obtained from the European Space Agency (ESA) Copernicus portal (<https://scihub.copernicus.eu>). The satellite image before the fire was selected in December 2018 and has less than 10 percent cloud cover and the satellite image after the fire was selected in March 2019 which from the report found that this month the most forest fires.

The 13 bands in Sentinel-2 products do not all have same resolution (therefore size) as mentioned in Table 8. Many operators do not support products with bands of different sizes so first we need to resample the bands to equal resolution. Define size of resampled product: By reference band from source product: B2, In this process, all the bands was resampled to 10 m resolution using bilinear interpolation, as suggested by Cansler (Cansler, 2011). Pixel sub-sampling methods of dNBR were compared between nearest neighbor, bilinear interpolation, and cubic convolution, They found that R^2 of bilinear interpolation is higher than other method. Bilinear interpolation is a common sampling approach for continuous data in which the resultant value is a weighted average of the four nearest pixel centroids, where closer pixel centroids are given higher weight than distant pixel centroids.

2. Burn area classification

In this study, the data used are the Sentinel- 2 satellite images, which consisted of 13 bands with a spatial resolution of 10, 20 and 60 meters. Sentinel-2 Level-2A product data were downloaded from the Copernicus Data Hub (ESA). Figure below: On December 26, 2018 (before the fire incident) and figure below: On March 31, 2019 (after- fire incident) in the dry or summer season which is the period of the occurrence of forest fires, shown in Figure 11. Next, Sentinel-2 images were resampled resolution to 10 meters pixel size for detect burn area and estimating aboveground biomass.

The images for this investigation were obtained from the Copernicus Data Hub of the European Space Agency (ESA) (<https://scihub.copernicus.eu/>) (ESA, 2015). In this study, Band 3,6,7,8,8A and 12 were used to create burned area map. The spatial resolution of these wavelengths will be different. Thus, these five bands were resampled into 10 meters. After resampling five bands to 10 meters, before-fire and post-fire images were calculated with NBR, RBR, BAIS2 indices using equation in Table 10 and finally these results, these results were compared with reference data.

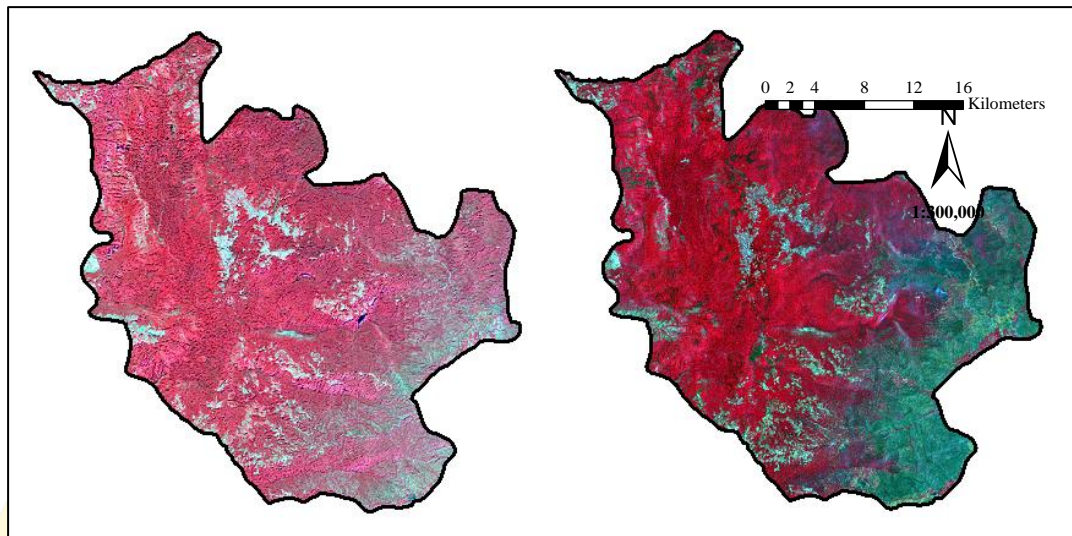


Figure 11 Pre-fire event on 26 December 2018 and Post-fire on 31 March 2019 image

(Red Green Blue, composite, 8 4 3)

3. Burn Classification accuracy

Binomial probability theory was used to assess the accuracy of the classified map of the burned area by the calculated sample size N . (Congalton & Green, 1998)

P - expected percent accuracy,

$q = 100 - p$

E - allowable error

$Z = 1.96$ (from the standard normal deviate of 1.96 for the 95% two-sided confidence level).

In this study, the expected accuracy is 80 percent and the allowable error is 10 percent. The equation below shows the calculation results. The minimum sample number is 61.46 checkpoints.

$$N = \frac{Z^2(p)(q)}{e^2} \quad (11)$$

$$N = \frac{1.96^2(80)(20)}{10^2} = \text{a minimum point of 62 points}$$

Thus, the minimum number of checkpoints must be at least 62 points. The study area was defined on the reference burn data by stratified random sampling method. A total of 70 checkpoints were chosen by stratified random sampling method in burned and unburned class.

4. Kappa coefficient

To check the accuracy of the image classification of the burned area, 140 checkpoints were used to assess the accuracy by Kappa coefficient. (Banko, 1998)

$$\hat{K} = \frac{M \sum_{i=j=1}^r n_{ij} - \sum_{i=j=1}^r n_i n_j}{M^2 - \sum_{i=j=1}^r n_i n_j} \quad (12)$$

Where:

r = number of rows in the error matrix

n_{ij} = number of observations in row i , column j

n_i = total number of observations in row i

n_j = total number of observations in column j

M = total number of observations in matrix

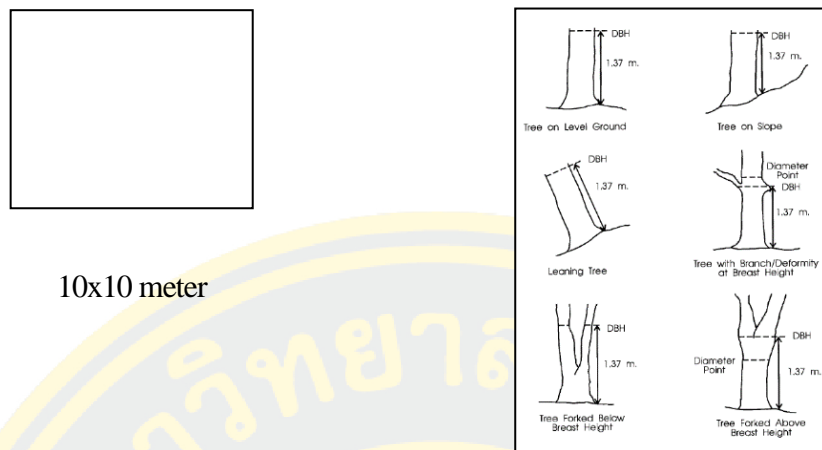
\hat{K} Values 0.61- 0.80 represent substantial agreement and \hat{K} values > 0.80 represent the strong agreement of accuracy between reference data and the burned map.

5. Field data collection

5.1 Sample design and field data collection

In this study, the sample plot size is 10 x 10 meters (square sample). 47 sample plots were used to collect tree at a height greater than or equal to 1.30 m and diameter at breast height (DBH) greater than or equal to 4.5 cm. Sample plot size is the same size of the image resolution (10 resolution) (L. Chen et al., 2018) (Figure 12).

In this study, deciduous forest areas were considered to calculate the loss of above-ground biomass which these areas occurred forest fire higher than another area. A total of 54 tree species were found in sample plots.



(Miller, Stolte, Duriscoe, & Pronos, 1996)

Figure 12 Square sample plot and standard method to measure the size of tree

5.2 Calculation of AGB estimation

The values of the biomass aboveground in deciduous forests were calculated using the equation allometric of forest type parameter that has studied previously. The allometric equation in this research was formulated by (Ogawa, 1965)

Table 13. Allometric Equation

Type	Equation	
Deciduous dipterocarp forest	$W_s = 0.0396 (D^2 H)^{0.9326}$	(13)
Mixed	$W_b = 0.003487 (D^2 H)^{1.0270}$	(14)
Deciduous forest	$W_l = [28.0 / (W_s + W_b) + 0.025]^{-1}$	(15)

Where Above-ground biomass = $W_s + W_b + W_l$ (Kilograms)

W_s = Stem biomass (Kilograms)

W_b = Branch biomass (Kilograms)

W_l = Leaf biomass (Kilograms)

D = Diameter at Breast Height (Centimeters), H = Height (Meters)

The allometric equation was developed in 1965 which studied on three main types of forest in Thailand. Many researchers in Thailand have used this equation because it is considered to be appropriate for estimating biomass in deciduous forest types.

6. Spectral indices of Sentinel-2 satellite image

Vegetation indices was chosen according to previous biomass estimates. For this study, only five indices will be chosen for biomass estimation. The formula is shown in Table 10. These analyzing steps will be performed using SNAP software.

6.1 NDVI

6.2 RENDVI Red-edge2

6.3 RERVI Red-edge2

6.4 GNDVI

6.5 NDI 45

7. Modeling the Relationship between Field AGB and Satellite Data

These analysis steps will be performed using SNAP software, ENVI, Microsoft Excel and AGB predictor by machine learning regression (Random Forests, Support Vector Machines for Regression will be processed in Spyder (Python 3.7) program The models defined the best parameters with the higher correlation coefficient (r), and the lower root means square error (RMSE) for the prediction of AGB, and finally, AGB mapping will be processed in ArcGIS, Qgis software.

In this study, five vegetation indices values were used as predictor variables combine with AGB in the field which calculated using the allometric equations in 47 sample plots. Finally, the Analysis relationship between AGB in plots and Vis value to predict biomass by machine learning regression. The step show AGB predictor using the machine regression model as follows:

In 47 sample plots, 33 sample plots were selected randomly for modeling (training data) and 14 sample plots were considered for validation data.

Independent variables are the vegetation indices and dependent variables are aboveground biomass. Vegetation indices values and aboveground biomass in 47 sample plots were prepared in an excel file for regression model analysis in Spyder (Python 3.7) program to acquisition the best regression model. The last step, Aboveground biomass loss map was generated by AGB optimal model.

8. Statistics analysis

The MSE, MAE, RMSE, and R-Squared metrics are mainly used to evaluate the prediction error rates and model performance in regression analysis.(Botchkarev, 2018)

MAE (Mean absolute error) shows the difference between the original and predicted values extracted by averaged the absolute difference over the data set.

MSE (Mean Squared Error) shows the difference between the original and predicted values extracted by squared the average difference over the data set.

RMSE (Root Mean Squared Error) is the error rate by the square root of MSE.

R-squared (Coefficient of determination) shows the coefficient of how well the values fit compared to the original values. The value from 0 to 1 interpreted as percentages. The above metrics can be expressed

$$MAE = \frac{1}{N} \sum_{i=1}^N |y_i - \hat{y}_i| \quad (16)$$

$$MSE = \frac{1}{N} \sum_{i=1}^N (y_i - \hat{y}_i)^2 \quad (17)$$

$$RMSE = \sqrt{MSE} = \sqrt{\frac{1}{N} \sum_{i=1}^N (y_i - \hat{y}_i)^2} \quad (18)$$

$$R^2 = \frac{\sum (y_i - \hat{y}_i)^2}{\sum (y_i - \bar{y})^2} \quad (19)$$

Where \hat{y} -predicted value of y, \bar{y} -mean value of y

4. EXPERIMENT RESULT AND DISCUSSION

Burn area classification

1. Differenced Normalized Burned Ratio (dNBR)

dNBR was calculated using NIR band and SWIR band which the value is -1.17- 1.53. The low values are healthy vegetation area and the high values are burned area. 35 hotspots were found in MODIS and 254 hotspots were found in VIIRS in burned area which is shown in Figure 13, Figure 14 and Figure 20. The area of the burn was approximately 110.25 Km², depicted in Table 14.

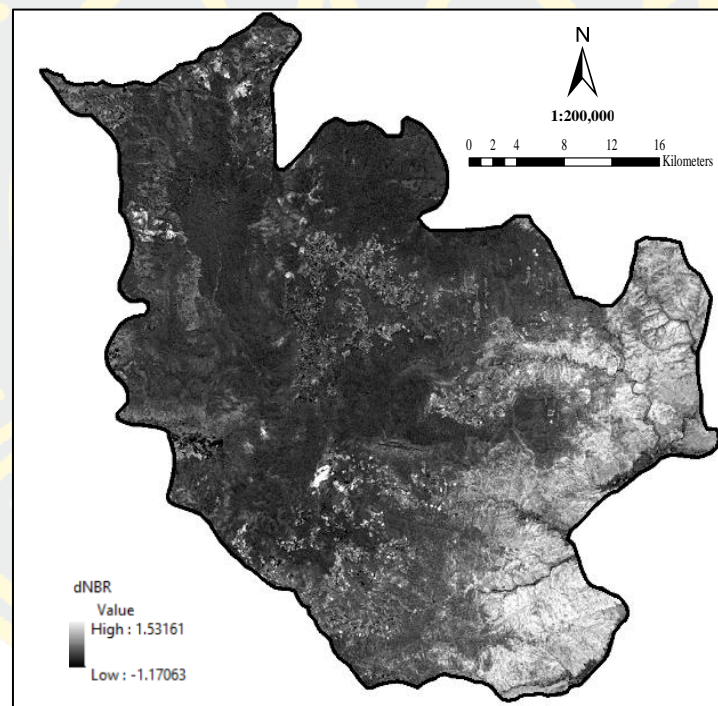


Figure 13 dNBR classification map

Table 14. Classification of burned area and unburned (dNBR)

Class	Area (Km ²)
Unburned	356.19
Burned	110.25
Total	466.45

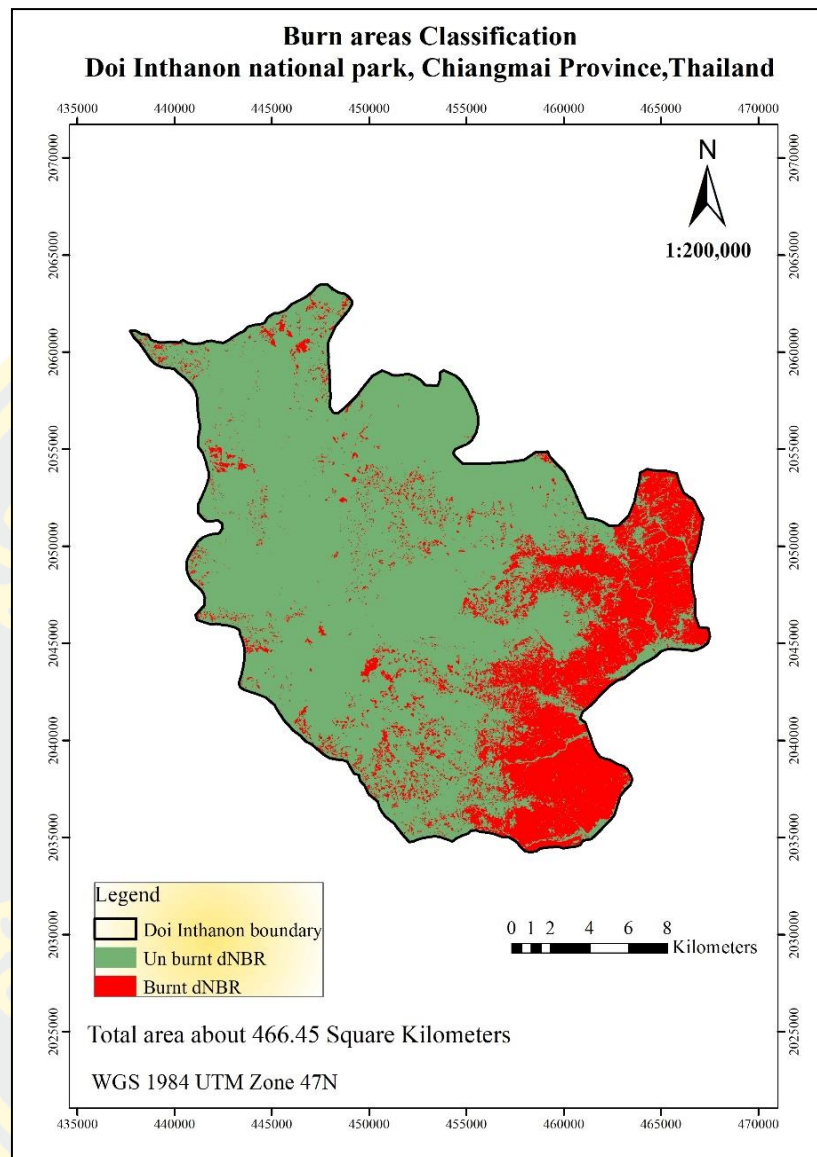


Figure 14 dNBR classification map

2. Relativized Burn Ratio (RBR)

The RBR value is $-2.05 - 0.99$. The low values are healthy vegetation area and the high values are burned area. The active fire hotspots were found in MODIS and VIIRS with 29 and 184 respectively in the burned area shown in Figure 15 and Figure 20.

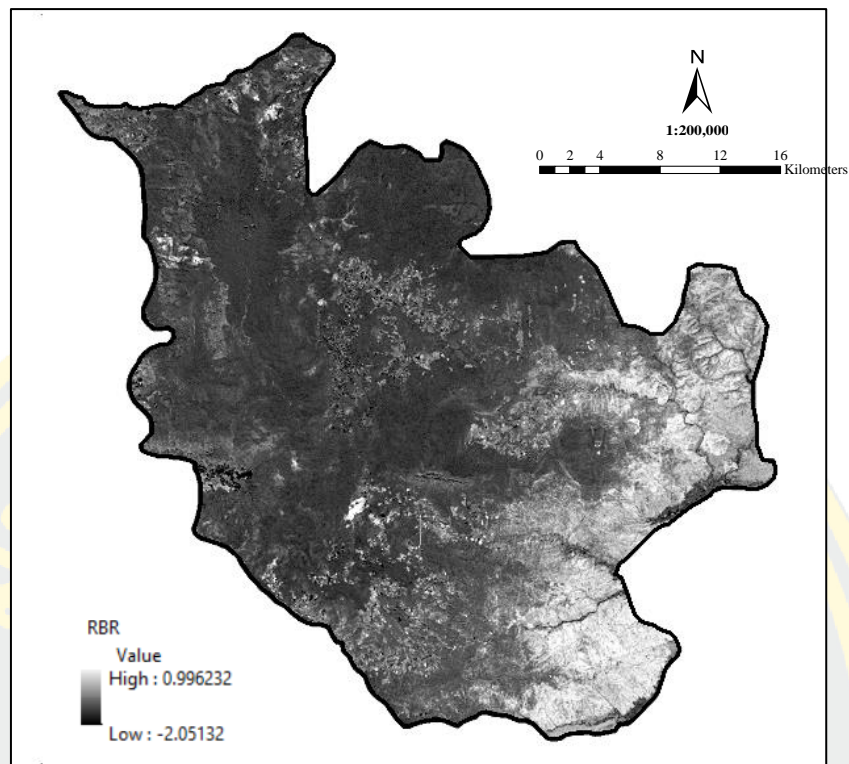


Figure 15 RBR classification map

Table 15. Classification of burned area and unburned (RBR)

Class	Area (Km ²)
Unburned	396.75
Burned	69.70
Total	466.45

Relativized Burn Ratio (RBR) map was generated by using equation (3) in Table 10 and if the value is greater than 0.27, then the class is burned otherwise un-burned (Parks et al., 2014). RBR is a strong metric for measuring and classifying burn severity over a broad range of fire-regime types. The area of burned was approximately 69.70 Km² shows in Table 15 and maps of RBR were generated in 2019 shown in Figure 16.

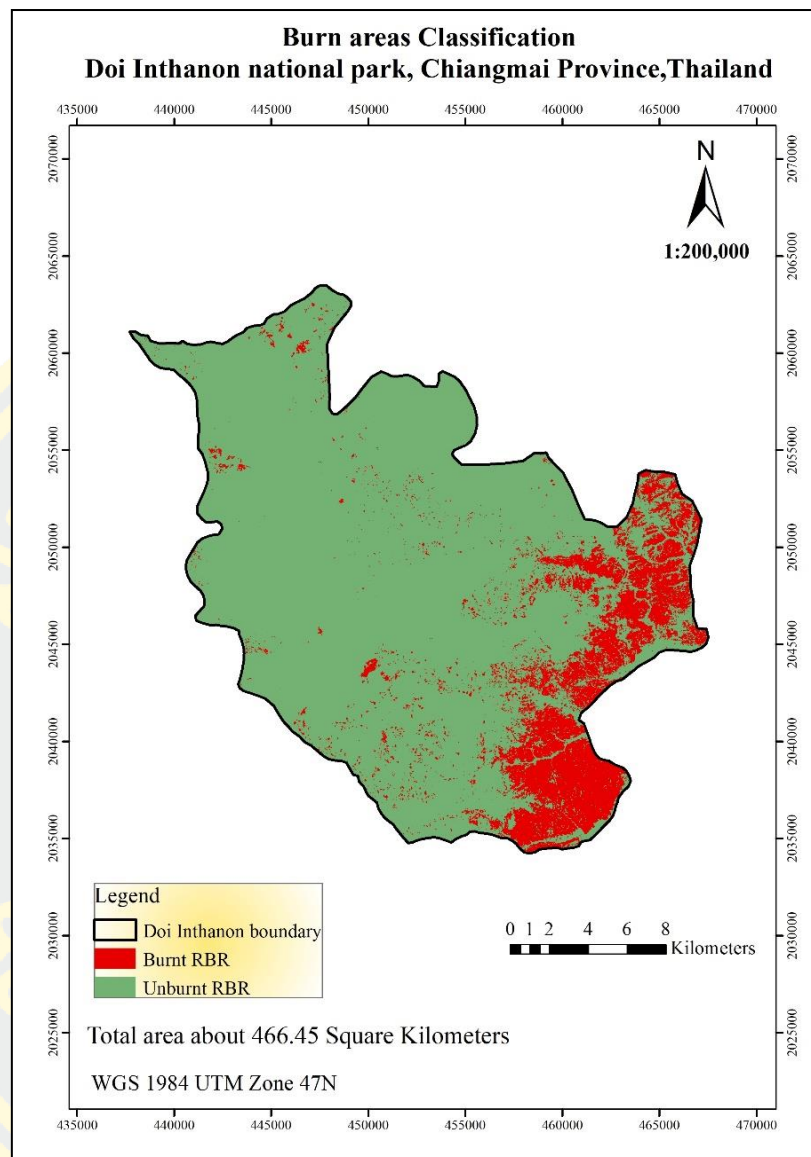


Figure 16 RBR classification map

After that, RBR was classified according to the United States Geological Survey (USGS) level, which is divided into seven levels. In the burn severity map, it was assumed that forest fires fell in low to high. Severity levels were categorized as a burned class and the rest of them are un-burned. Burned severity maps of RBR were generated in 2019 shown in Figure 22

3. Burned Area Index for Sentinel-2 (BAIS2) Classification

The BAIS2 value is ranged from -2.05 – 0.99. The low values are healthy vegetation area and the high values are burned area. It was found 29 and 184 of MODIS and VIIRS active fire hotspots respectively in the burned area.

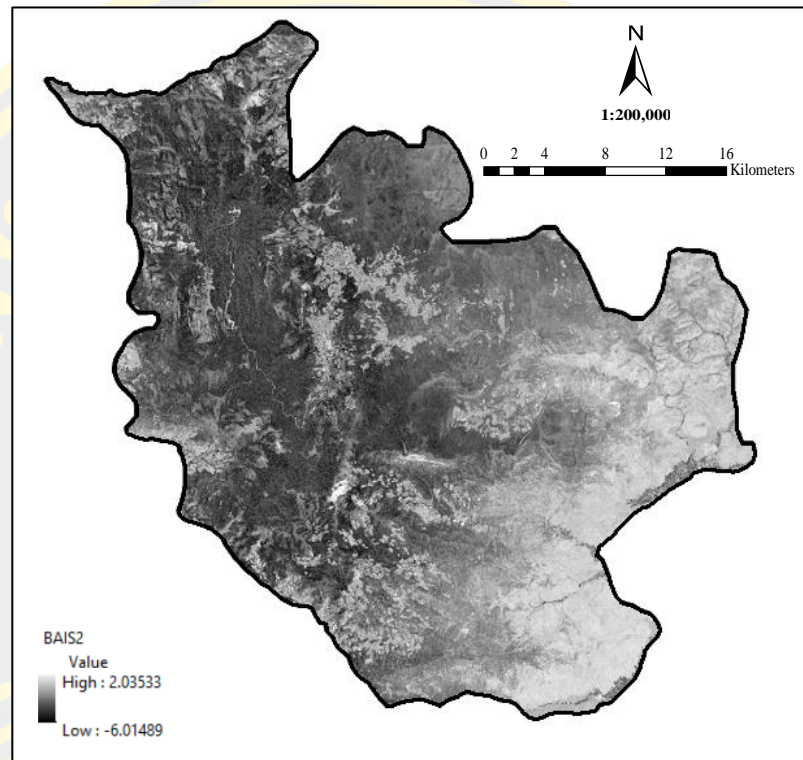


Figure 17 BAIS2 classification map

The burning area was approximately 48.91 Km² shown in Table 16 and Maps of BAIS2 were generated in 2019 shown in Figure 17 and Figure 18. MODIS and VIIRS active fire hotspots were found at 22 and 135 points, respectively.

Table 16. Classification of burned area and unburned (BAIS2)

Class	Area (Km ²)
Unburned	417.54
Burned	48.91
Total	466.45

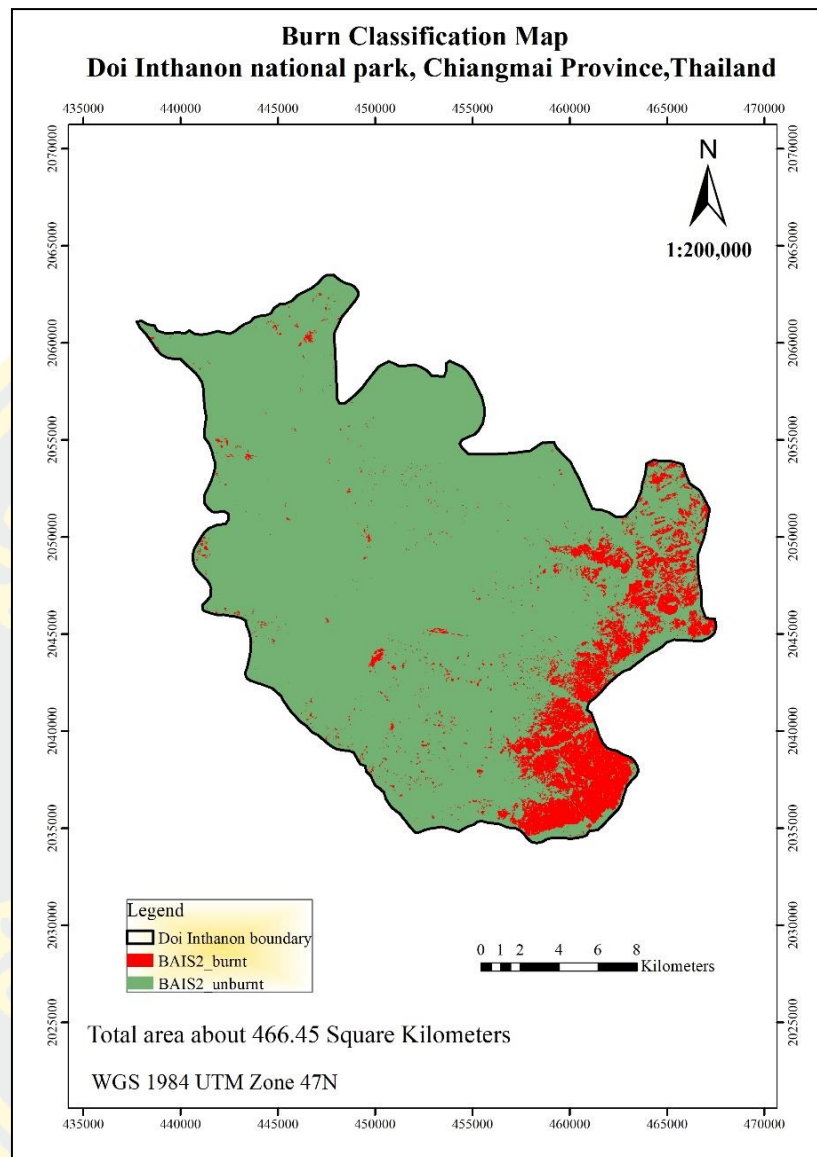


Figure 18 BAIS2 classification map

4. Burned area published GISTDA (referenced data)

GISTDA has analyzed and calculated the burned scar (burned scar) by using difference Normalized Burn Ratio (dNBR) which is derived from the LANDSAT-8 satellite image in 2019 using images of different time periods, these images were analyzed the relationship between pre-fire even and post-fire event and Near-Infrared band, Shortwave Infrared band were used to classified the burned area. The area of burned was approximately 56.90 Km² shown in Table 17 and Maps of reference data were

generated in 2019 shown in Figure 19 and 28 hotspots were found in MODIS and 156 hotspots were found in VIIRS in burned area shows in Figure 20.

Table 17. Classification of burned area and unburned (reference)

Class	Area (Km ²)
Unburned	409.55
Burned	56.90
Total	466.45

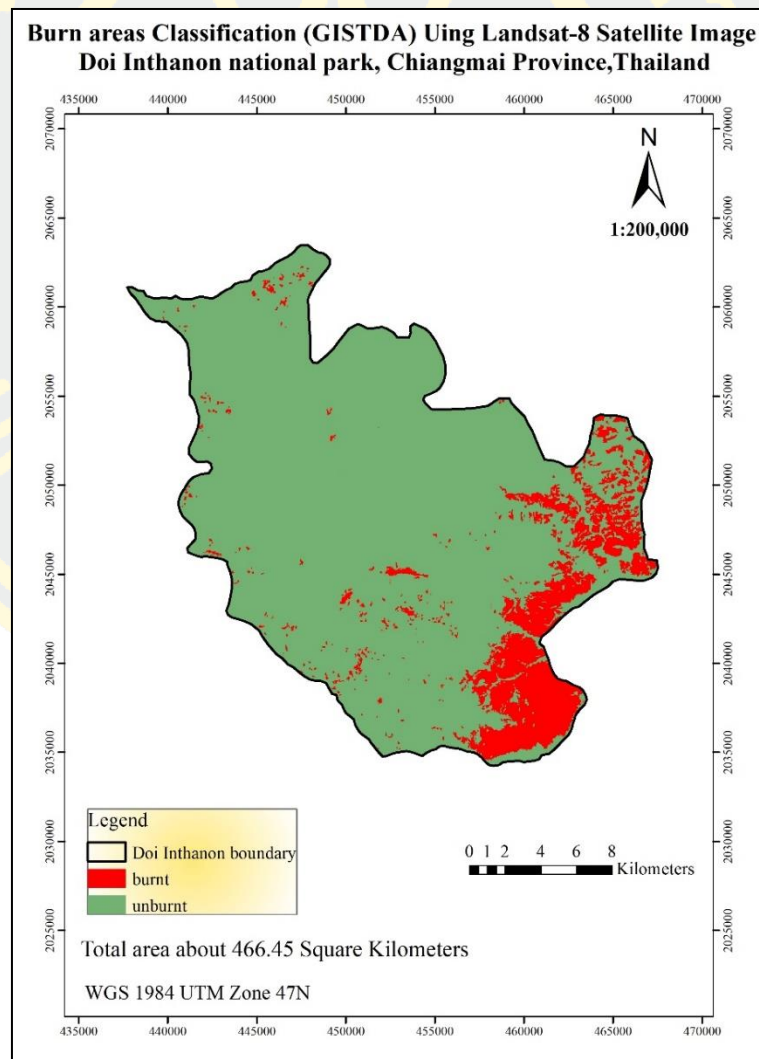


Figure 19 Reference classification map

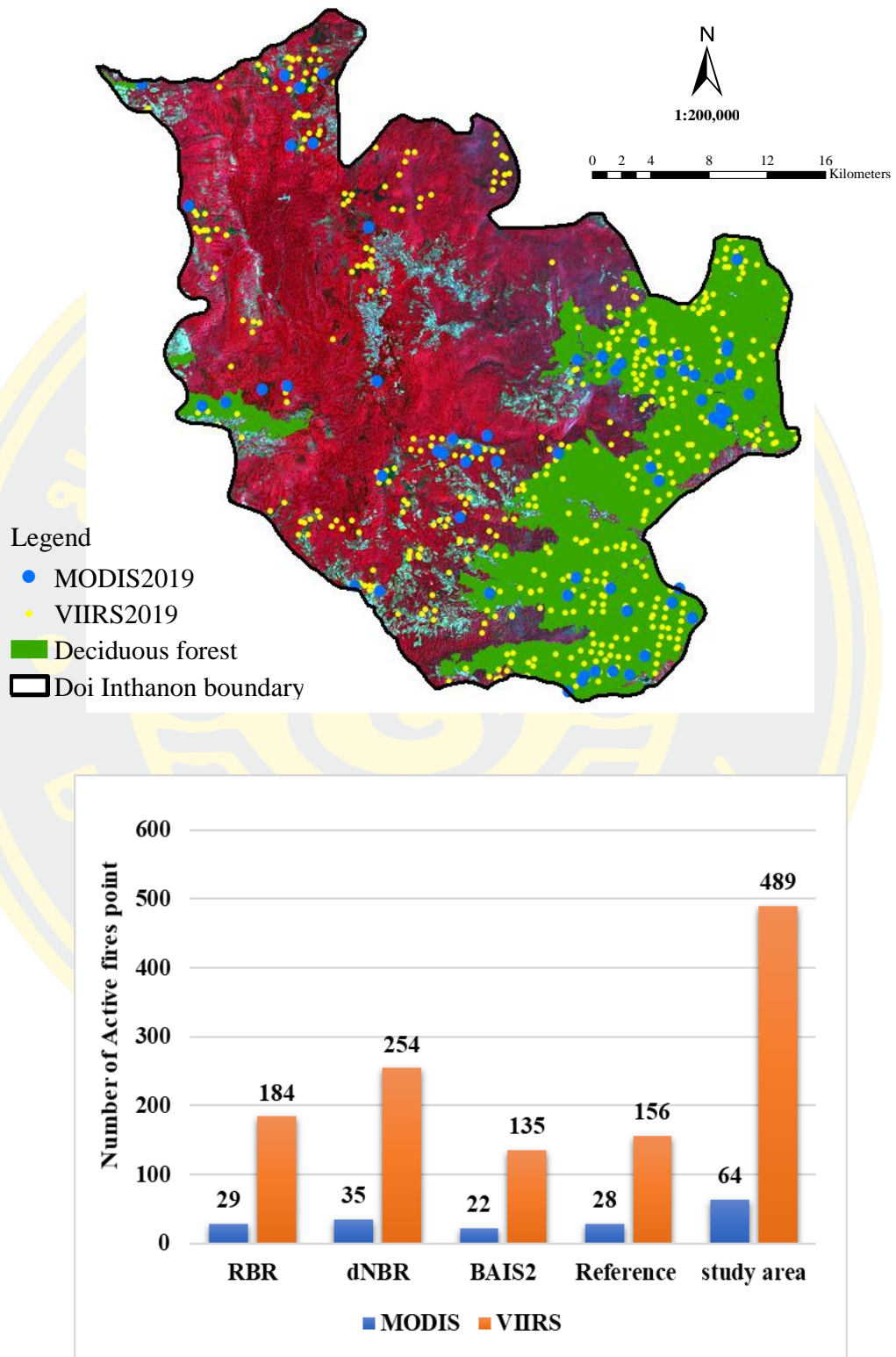


Figure 20 Map of the main forest types affected by fires and comparison of the number of active fire hotspots in burned class

Burn Classification accuracy and Burn severity map

Table 18. Accuracy assessment

Burn Index	Reference data (GISTDA)		
Classes	Burned	Unburned	Total
RBR			
Burned	58	2	60
Un burned	12	68	80
Total	70	70	140
Overall accuracy (%)	90.00	Kappa Index	0.81
BAIS2			
Burned	55	3	58
Un burned	15	67	82
Total	70	70	140
Overall accuracy (%)	87.14	Kappa Index	0.75
dNBR			
Burned	58	14	72
Un burned	12	56	68
Total	70	70	140
Overall accuracy (%)	81.43	Kappa Index	0.64

The Results of the classification of the burn area were compared with the burn area that has been published by the Geo-informatics Technology Development Agency (GISTDA) of Thailand, shown in Table 18 and Figure 23

The Result shows that the RBR classification mapped with high accuracy : 90.00% overall agreement with the reference map and the kappa coefficient is 0.81.

The area of the burned area was found around 69.70 square kilometers of the study area. The burn area of RBR was classified by burn severity levels of USGS in Table 9, if the value is greater than 0.27 then the class is burned otherwise unburned (Parks et al., 2014; Suresh Babu et al., 2018).

In this research, The thresholding value of the burned area is 0.27 – 0.99. Thus, burn severity map was classified 4 class (unburned, moderate to high severity level according to the burn severity classes in Table 9) which it was found that most of the area is in the Moderate-Low Severity level (Figure 22).

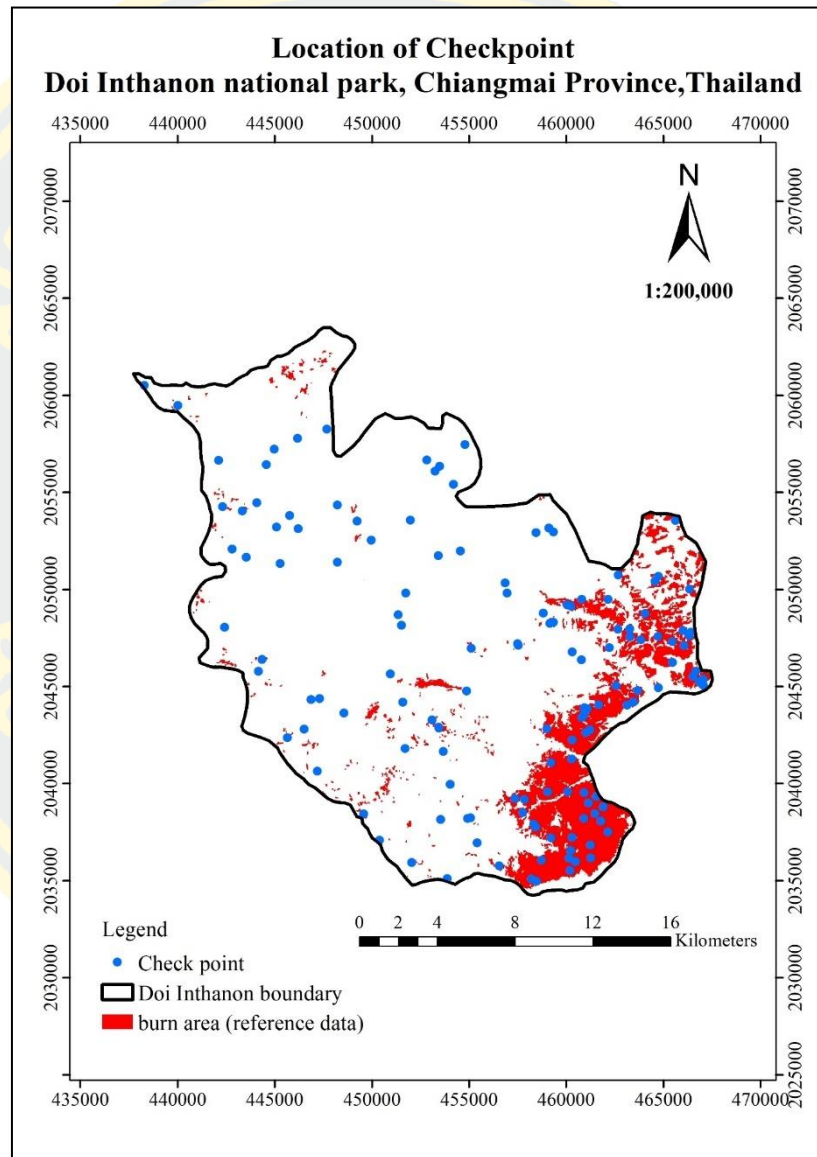


Figure 21 Location of checkpoints in the study area

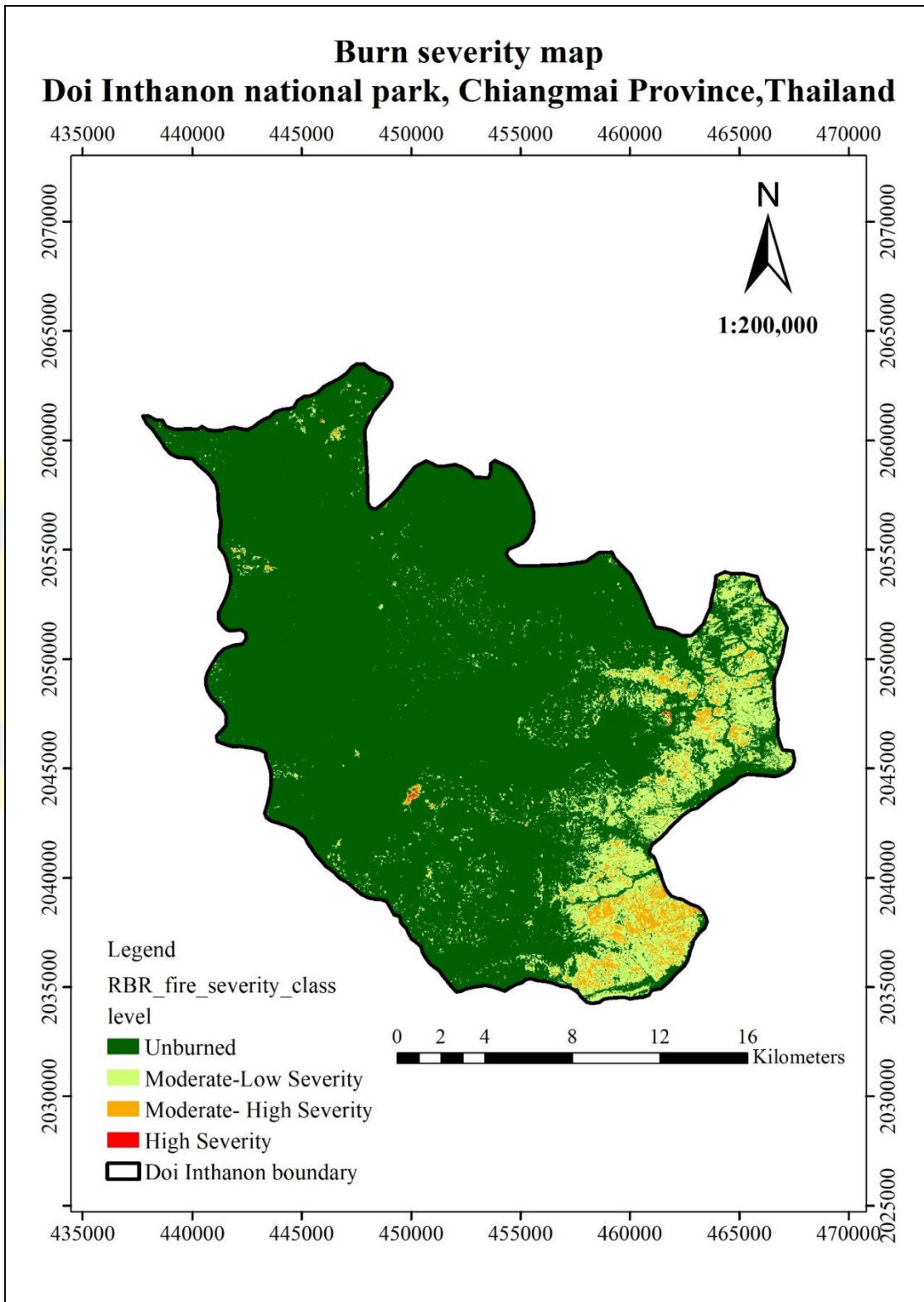


Figure 22 Burn severity map of RBR

From the result of the BAIS2 classification map, the present overall accuracy is 87.14% and the kappa coefficient is 0.75. In this study, The BAIS2 value was determined according to the study of Federico Filipponi (Filipponi, 2018) who examined the map burned in the Messina, Italy. He also found that the burn area value of this index is in the range 0.75 - higher than 1. Therefore, the BAIS2 index in this study was determined just as the previous research. Finally, the result of dNBR map is quite different from the two indices. The percentage of overall accuracy is 81.43% and the kappa coefficient is 0.64 which represents a moderate agreement between the classification map and the reference information.

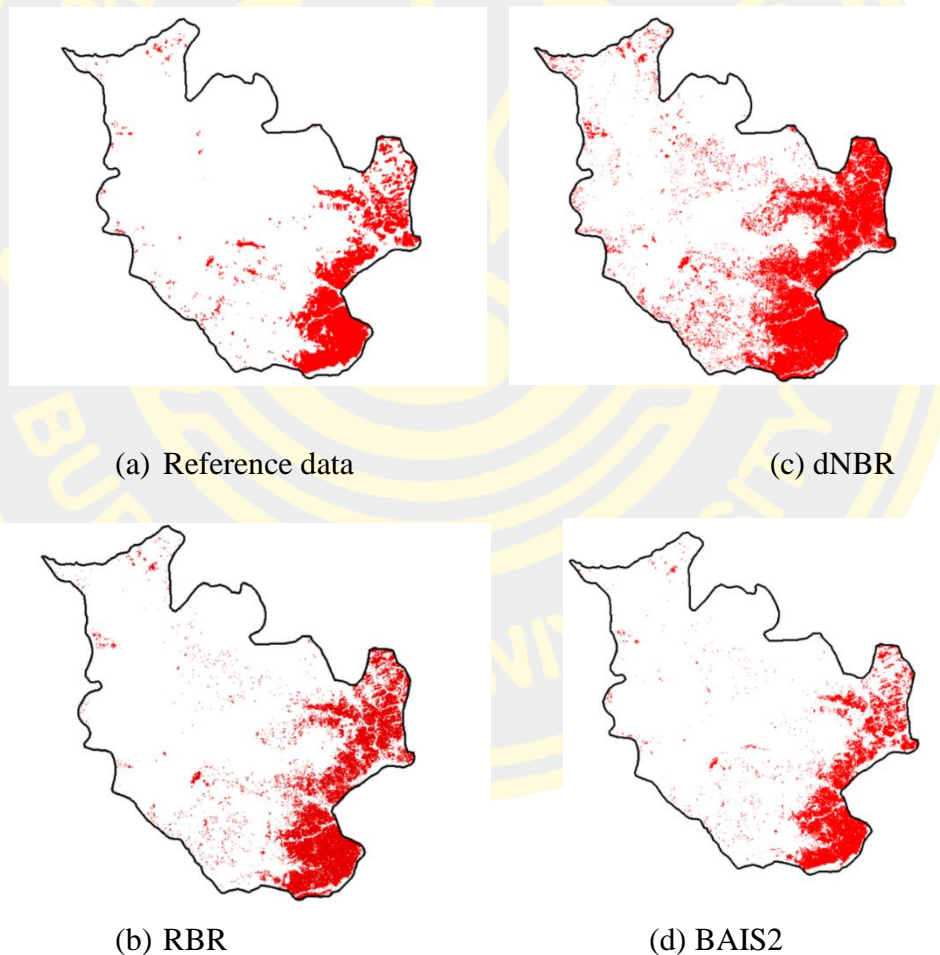


Figure 23 Comparison of Burned map

In terms of forest type affected by the fires, The major fire-affected area is in lowland in the study area, especially in the dry dipterocarp and mixed deciduous forest. Active fire hotspots were found in these areas about 553 points shown in Figure 20.

From this study, it represents that Sentinel-2 Satellites are useful in evaluating burned areas or the area that is damaged by fire. Therefore, the burn severity map can help manage fire events quicker than Landsat Satellites.

Above ground biomass estimation

1. Calculation of Vegetation Indices using Sentinel-2 satellite image

The Vis indices were calculated using band math in SNAP software. All five indices were computed using the equation in Table 10. The indices are NDVI, RENDVI Red-Edge 6, RERVI, GNDVI and NDI45. The five results image shown in Figure 24.

In this study, we focused on deciduous forest area which forest fire occurred higher than another area. Moreover, the active fire hotspots were found almost all over the area.

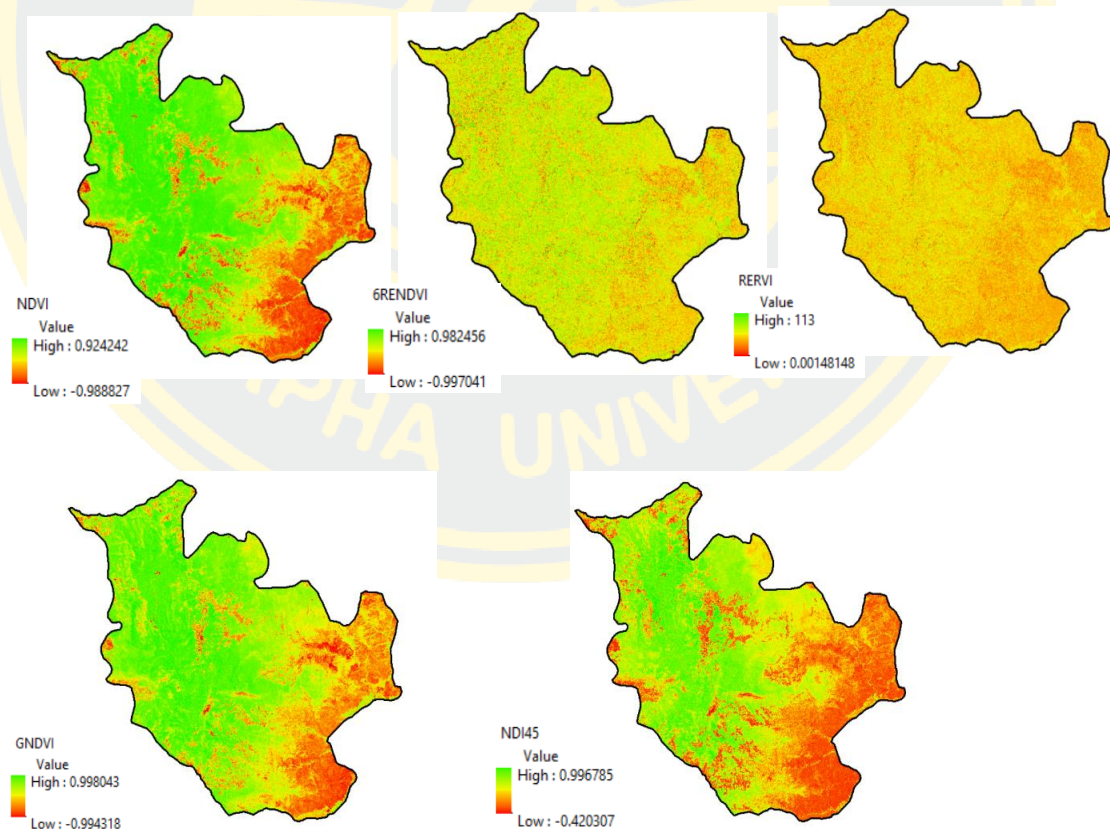


Figure 24 Vegetation Indices (VIs) using Sentinel-2 optical satellite image

2. Calculation of AGB from field measurement

AGB was described as the sum of stem, branches, leaves biomass. The tree height and DBH data were used to calculate ws, wb, wl and total of AGB using the allometric equation shown in the Table 19.

Table 19. Descriptive of Above ground biomass estimation from field measurement. total of 47 plots

Plot No.	Ws(kg)	Wb(kg)	Wl (kg)	AGB (kg)	AGB (Mg/ha)
1	1382.95	404.60	34.67	1822.22	182.22
2	953.25	191.23	34.17	1178.65	117.86
3	1069.81	215.27	38.83	1323.91	132.39
4	1425.48	439.97	28.36	1893.81	189.38
5	1106.76	230.06	38.31	1375.13	137.51
6	480.29	88.45	18.74	587.49	58.75
7	213.45	37.56	8.54	259.55	25.95
8	817.32	168.74	28.35	1014.41	101.44
9	734.39	132.68	29.08	896.15	89.62
10	934.54	182.90	34.83	1152.27	115.23
11	569.51	105.67	22.30	697.49	69.75
12	750.28	151.53	26.47	928.27	92.83
13	846.30	158.32	32.83	1037.44	103.74
14	544.65	98.18	21.70	664.54	66.45
15	338.69	58.71	13.64	411.04	41.10
16	344.74	57.64	13.99	416.36	41.64
17	440.05	88.36	15.35	543.76	54.38
18	448.50	79.36	17.77	545.62	54.56
19	1485.89	333.81	42.30	1861.99	186.20
20	1511.91	317.17	50.67	1879.76	187.98
21	620.82	112.69	24.46	757.98	75.80
22	795.53	165.81	26.13	987.47	98.75
23	1304.46	373.69	35.25	1713.41	171.34
24	696.60	132.08	27.05	855.73	85.57
25	573.36	108.20	22.20	703.76	70.38
26	230.48	40.61	9.22	280.31	28.03

Plot No.	Ws(kg)	Wb(kg)	WI (kg)	AGB (kg)	AGB (Mg/ha)
27	787.16	158.33	28.60	974.09	97.41
28	1639.83	336.27	58.31	2034.41	203.44
29	722.94	140.51	27.16	890.61	89.06
30	355.65	63.85	14.19	433.69	43.37
31	745.57	146.30	27.23	919.10	91.91
32	680.86	138.25	23.91	843.01	84.30
33	1132.80	265.37	27.44	1425.62	142.56
34	930.57	178.98	35.54	1145.09	114.51
35	438.88	82.75	16.86	538.49	53.85
36	349.07	60.56	14.04	423.67	42.37
37	375.91	64.83	15.20	455.94	45.59
38	1192.57	263.28	35.37	1491.22	149.12
39	822.52	157.68	31.49	1011.70	101.17
40	494.39	91.85	19.24	605.48	60.55
41	456.03	78.98	18.34	553.35	55.34
42	944.12	199.74	31.37	1175.23	117.52
43	207.79	35.37	8.38	251.55	25.15
44	861.21	179.89	28.38	1069.48	106.95
45	1343.24	277.71	47.04	1667.99	166.80
46	1448.87	296.69	51.77	1797.34	179.73
47	822.73	164.77	29.19	1016.69	101.67
Total	37,372.73	7,855.264	1,284.268	46,512.277	4,651.23

3. The Value of Vegetation indices in deciduous forest sample plot

The vegetation indices were calculated using band math in SNAP software. All five indices were computed using the equation in Table 10 and the value shown in Table 20

Table 20. Value of Vis indices in plot

Plot No.	Location		NDVI	NDVI Red Edge	RVI Red Edge	GNDVI	NDI45
1	462303	2049950	0.428	0.109	1.245	0.093	-0.352
2	464236	2046476	0.379	0.176	1.429	-0.006	-0.567

Plot No	Location		NDVI	NDVI Red Edge	RVI Red Edge	GNDVI	NDI45
3	464213	2046504	0.350	0.123	1.281	-0.084	-0.498
4	464399	2046394	0.481	0.152	1.359	0.056	-0.405
5	465019	2045440	0.337	0.149	1.351	0.092	-0.506
6	465564	2045596	0.242	0.063	1.135	-0.172	-0.516
7	465715	2045540	0.205	0.101	1.226	-0.252	-0.653
8	465765	2045481	0.254	0.179	1.435	-0.005	-0.599
9	461445	2039888	0.277	0.072	1.155	-0.182	-0.510
10	461400	2039890	0.315	0.083	1.180	-0.185	-0.453
11	461206	2039758	0.249	0.078	1.170	-0.219	-0.552
12	461192	2039682	0.269	0.061	1.131	-0.202	-
13	461131	2039508	0.305	0.062	1.132	-0.178	0.537
14	461125	2039448	0.246	0.084	1.183	-0.241	-0.511
15	461117	2039387	0.218	0.086	1.188	-0.202	-0.562
16	460742	2038677	0.219	0.078	1.169	-0.240	-0.583
17	460696	2038630	0.237	0.065	1.139	-0.176	-0.588
18	460652	2038630	0.237	0.065	1.139	-0.176	-0.566
19	460652	2038702	0.238	0.068	1.147	-0.217	-0.578
20	457492	2038713	0.433	0.097	1.214	-0.109	-0.464
21	457469	2038733	0.469	0.135	1.313	-0.004	-0.433
22	457512	2038647	0.299	-0.008	0.984	-0.204	-0.498
23	457497	2038596	0.285	0.084	1.182	-0.213	-0.573
24	457426	2038600	0.336	0.103	1.229	-0.125	-0.498
25	457333	2038566	0.267	0.084	1.185	-0.185	-0.601
26	461430	2039973	0.226	0.077	1.168	-0.187	-0.526
27	461424	2039998	0.210	0.085	1.185	-0.174	-0.561
28	461162	2039810	0.280	0.045	1.094	-0.196	-0.528
29	461141	2039772	0.487	0.008	1.015	-0.119	-0.235
30	461049	2039543	0.232	0.056	1.119	-0.264	-0.591
31	460995	2039547	0.251	0.080	1.174	-0.221	-0.609
32	460671	2038793	0.276	0.155	1.366	0.008	-0.519
33	460681	2038810	0.254	0.135	1.313	-0.125	-0.620
34	457568	2038785	0.352	0.066	1.142	-0.013	-0.463
35	457555	2038771	0.313	0.091	1.200	-0.077	-0.466
36	458028	2038657	0.243	0.074	1.160	-0.252	-0.563
37	458012	2038654	0.223	0.074	1.159	-0.267	-0.637

Plot No	Location		NDVI	NDVI Red Edge	RVI Red Edge	GNDVI	NDI45
37	457984	2038644	0.231	0.080	1.175	-0.283	-0.651
38	457937	2038656	0.359	0.091	1.201	-0.201	-0.554
39	457922	2038679	0.292	0.043	1.089	-0.247	-0.597
40	458002	2038587	0.268	0.087	1.190	-0.186	-0.546
41	458015	2038604	0.240	0.087	1.190	-0.182	-0.599
42	465823	2046016	0.320	0.154	1.365	0.1439	-0.439
43	465735	2045620	0.200	0.032	1.065	-0.223	-0.553
44	465749	2045474	0.306	0.127	1.291	0.0309	-0.440
45	465304	2045384	0.364	0.162	1.387	0.0094	-0.459
46	465072	2045461	0.382	0.112	1.251	0.011	-0.455
47	465154	2045374	0.304	0.122	1.279	-0.018	-0.481

4. Aboveground biomass modelling, Statistical analysis

Remote sensing data from Sentinel -2 was used to estimate the AGB predictor under the random forest regression (RFR) and support vector regression (SVR). In this study, 33 out of the 47 plots were selected randomly for modeling and the remaining 14 plots were employed for validation of the model. In each model, the vegetation indices were selected to be independent variables(X) and above ground biomass was the dependent variable(Y), these variables were processed in Spyder Python software using the 6-fold cross-validation.

The Multiple linear regression, Random forest and Support vector machine were used to determine the optimal independent variables, including spectral variables, with respect to Response variable- the aboveground biomass from field measured. Vegetation indices were extracted at location of sample plot in field.

4.1 Statistical analysis of Total AGB (Ws+Wb+WI)

The Table 21 represents the accuracies of three model for estimate the AGB of 47 sample plots. The MAE value of model, it was lower with RF (4.17 Mg ha) and higher the other model ranging from 12.16 (Linear regression) to 38.69 Mg ha⁻¹ (SVR). The values of RMSE is range from 6.04 (RF) to 48.45 (SVR) Mg ha.

The RMSE values of RF is the lower than with other methods. For coefficient of determination, the relationship between observed and predicted biomass demonstrated, SVR 0.021 whereas linear regression and RF are 0.897, 0.984, respectively.

Table 21. Performance estimation of SVR and RF models.

Evaluation Index	Linear regression	SVR	RF
MSE	245.94	2347.23	36.51
MAE	12.16	38.69	4.17
RMSE	15.68	48.45	6.04
R-square	0.897	0.021	0.984

(Mean Squared Error, Mean Absolute Error, Root Mean Squared Error, Coefficient of determination are MSE, MAE, RMSE, R^2 , respectively.)

The RF model is the lowest RMSE and the highest coefficient of determination is R^2 value the closest-to-one values. Hence, in this study, the RF model was the most accurate model for estimating AGB. Besides, the accuracy ranking of the two model from low to high was SVR, linear regression, and RF.

From the field data surveys in the study area, it was found that most of the mixed deciduous forest and deciduous forest in the leaves of the trees are the most burned and loss parts. Therefore, the relationship of Aboveground biomass of leaves was analyzed in this study.

4.2 Statistical analysis of AGB leaves (W1)

Table 22. Performance estimation of SVR and RF models.

Evaluation Index	Linear regression	SVR	RF
MSE	0.32	0.605	0.077
MAE	0.45	0.605	0.198
RMSE	0.566	0.778	0.277
R-square	0.742	0.523	0.939

The Table 22 above represents the accuracies of three model for estimate the AGB(W1) of 47 sample plots. The MAE value of model RF, SVR, linear regression are 0.198, 0.605, 0.45 Mg ha, respectively. The values of RMSE ranges from 0.277 (RF) to

0.778 (SVR) Mgha. For coefficient of determination, the relationship between observed and predicted biomass demonstrated, RF 0.939 whereas linear regression and SVR are 0.742, 0.523, respectively.

5. Result of AGB mapping by Machine Learning regression model

5.1 AGB(Ws+Wb+Wl) mapping in burned area

The AGB predicted value was generated at 10 metres spatial resolution using RF model with five indices variables and the range of AGB(Wl+Wb+Ws) distribution from 28.73 to 191.98 Mg ha. The average predicted AGB loss was 108.815 Mg ha. shown in Figure 25

5.2 AGB(Wl) mapping in burned area

The AGB leaves predicted value was generated at 10 metres spatial resolution using RF model with five indices variables and the range of AGB(Wl) distribution from 0.86 to 53.33 Mg/ha. The average predicted AGB of leaves loss was 2.91 Mg ha. shown in Figure 26

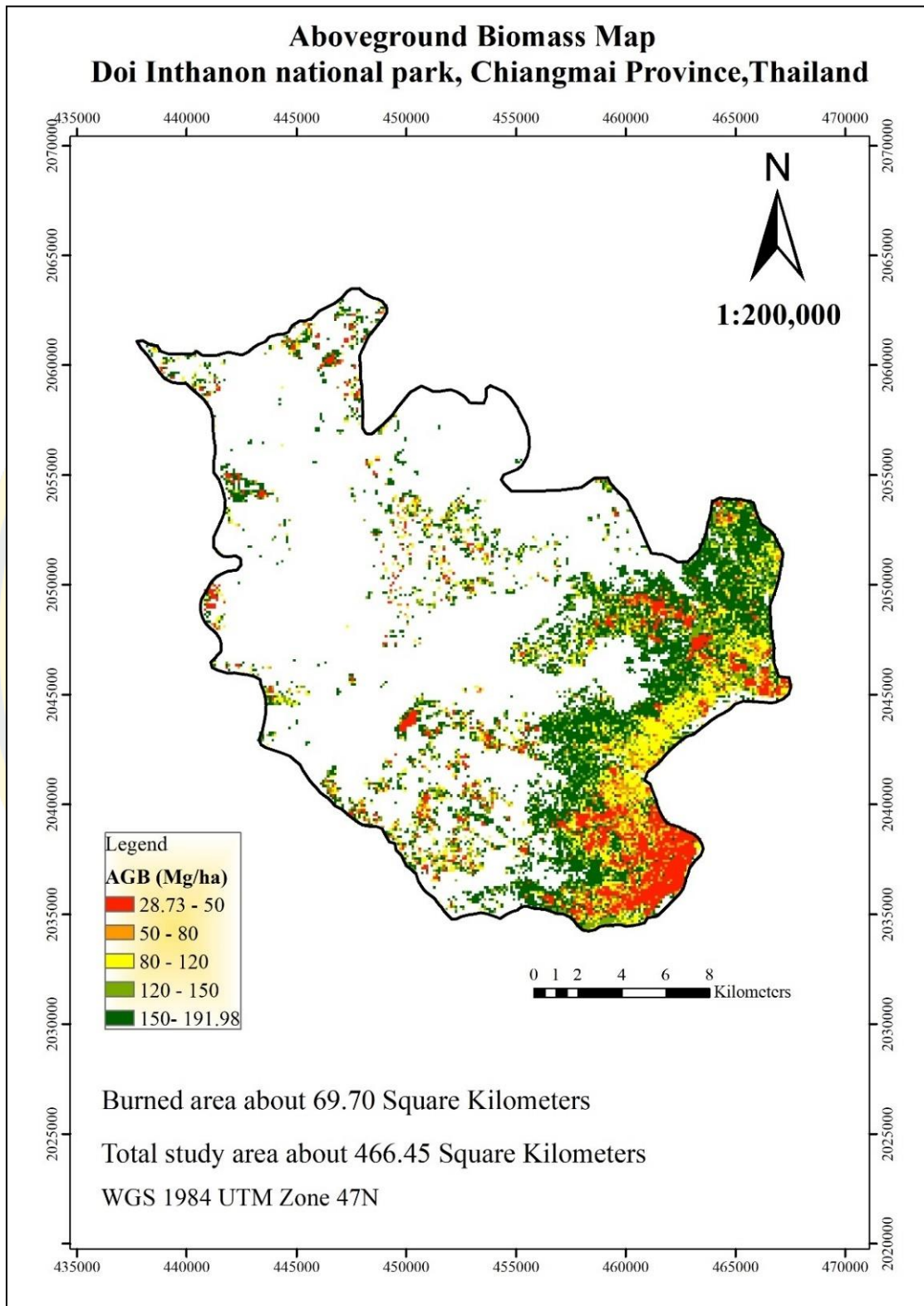


Figure 25 AGB predicted distribution in burned area

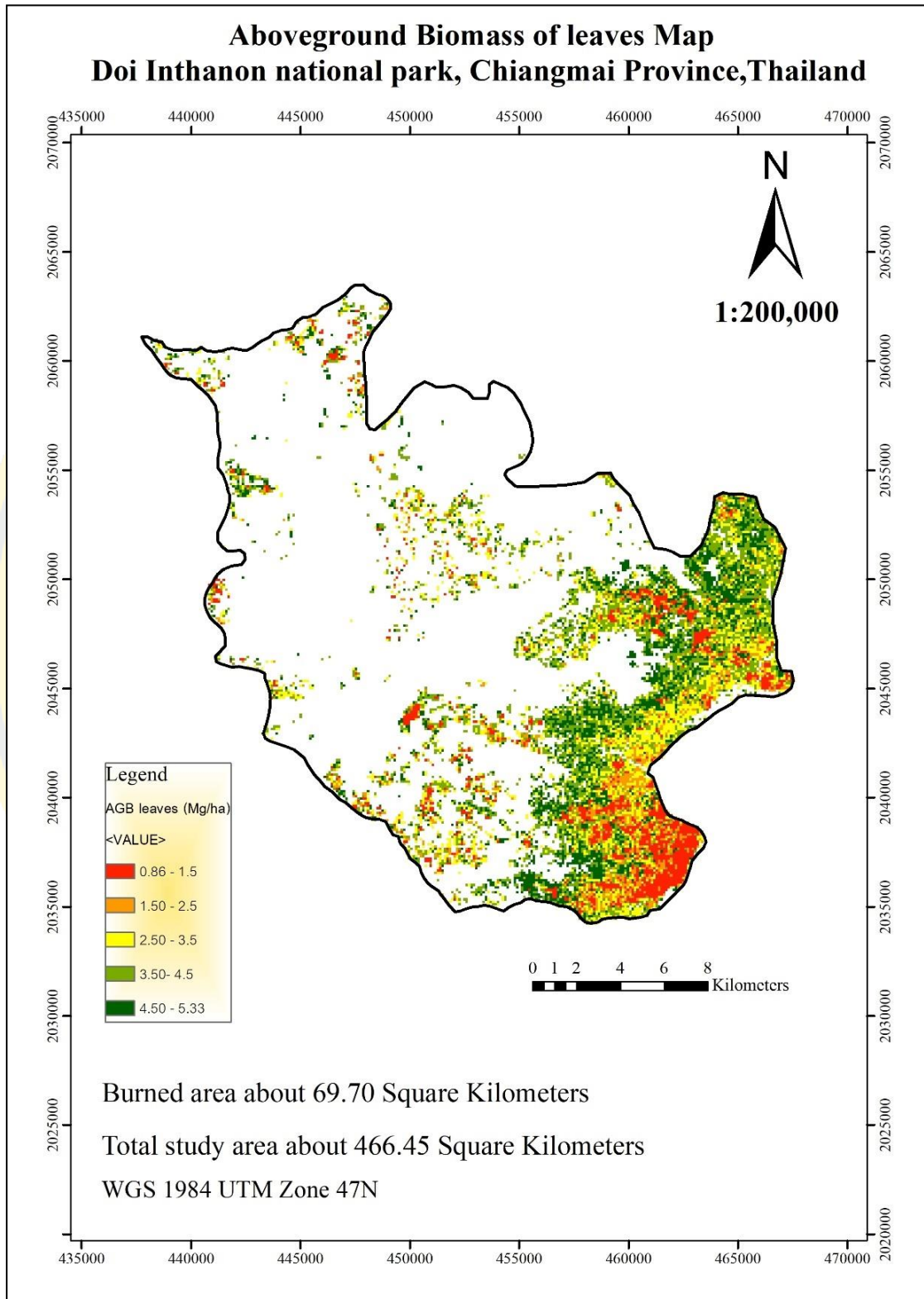


Figure 26 AGB of leaves predicted distribution in burned area

Discussion

The result shows that RBR is the best performance for assessing of burn area in this study. The RBR index results generally showed similar trends with reference data and the accuracy is higher than BAIS2 and dNBR indices. It is also consistent with the study of Suresh Babu et al. (2018). Similarly, BAIS2 index's performance is quite good and it is a newly developed index for the Sentinel-2 satellite image.

Moreover, it is able to analyze the area which is expected to be burned by using the only image after the fire. However, the equations are more complicate than the indices mentioned above. The dNBR index shows results differently from reference data. The difference might be from the timing of the satellite images before and after the fire event that is extremely important. Moreover, the result of the classification of burned area map was analyzed combined with active fire hotspot that have been conducted by the FIRMS. Analysis results show that the burn area will have the number of hotspots higher than the unburned area.

This result is in accordance with previous experiments of Park et al. (2014) that demonstrated that RBR is a robust metric for measuring and classifying burn severity. Although RBR index was used to classify burn severity for Landsat- Satellite-based but the result in the present study, it also indicated that RBR index can be used with Sentinel-2 satellite image.

In addition, the result of the BAIS2 index shows that it is quite a good performance for burned area mapping. The result is consistent with Filipponi's (2018) study which indicates that BAIS2 showed a good performance of BAIS2 for the detection of burned areas when compared with NBR index and it can identify small burned areas at 20-meter spatial resolution of Sentinel-2 satellite.

After that, the burned area as mention above was used to consider for estimating aboveground biomass loss. In the present study, the RF model shows the best statistical values when compared to other methods. Since it is a very stable random method. Although the data of some variables or parameters that are not linear does not affect the efficiency of the Random Forest.

The result is consistent with the study of Chrysafis et al.,2017 ; Dang et al., 2019 ; Pandit et al., 2018 ; which represents that RF regression model shows the high coefficient of determination and The results found in this study represent that Sentinel-2

image combined with RF regression model has the potential to effectively predict the spatial distribution of forest AGB with adequate accuracy.

From Table 23 show summarizes previous studies in other study areas that use the machine learning method to assess biomass. Machine learning, such as RF SVM, is used to assess the accuracy of biomass assessments in different terrain and ecosystems.

The results of their research show that the use of machine learning techniques combined with remote sensing and field survey data has a high potential for biomass assessment. This demonstrates the potential of machine learning techniques such as RF for estimate AGB with high accuracy. As compared to linear modeling.

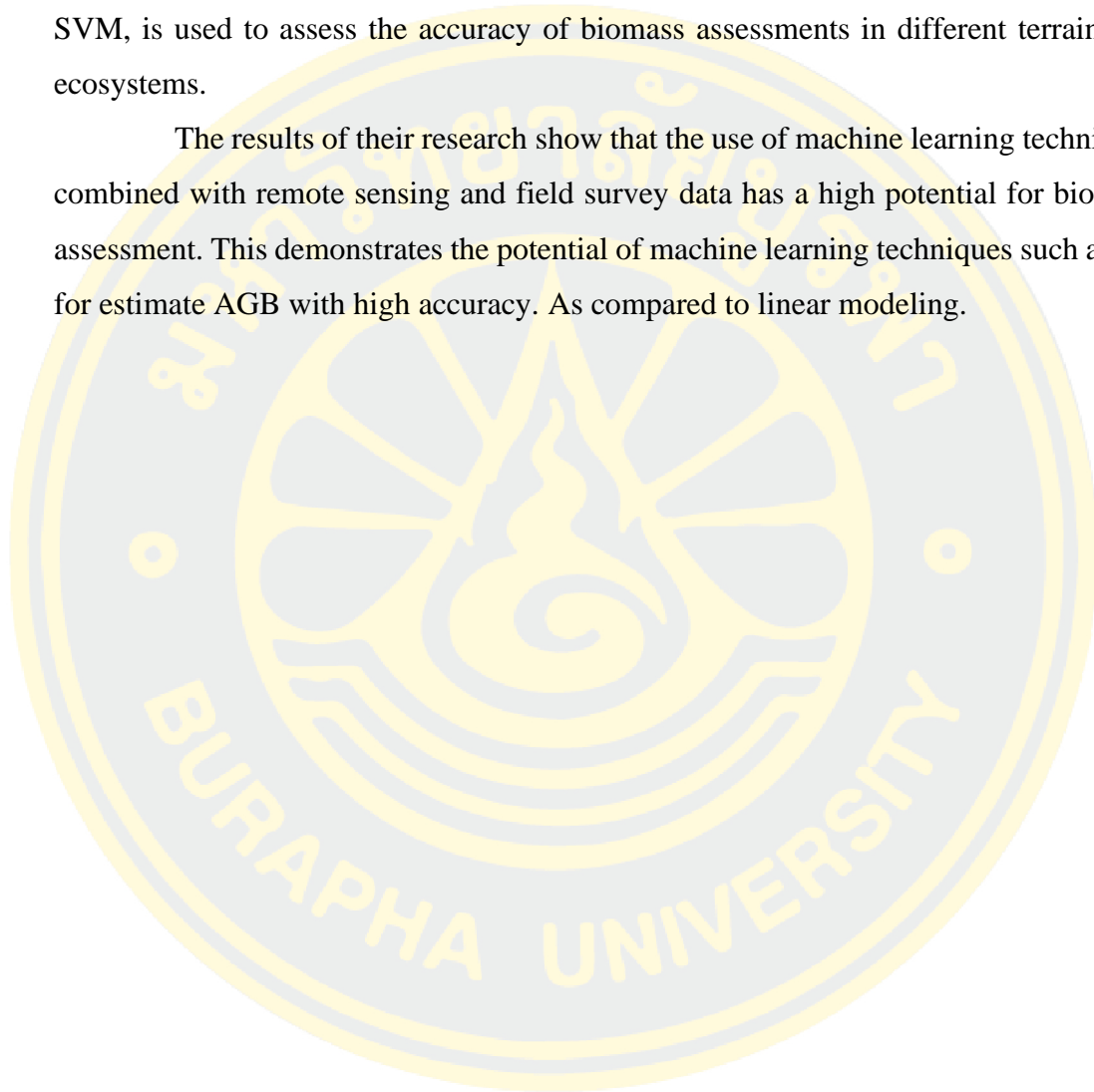


Table 23. Comparison of previous studies with machine learning

No.	Modelling	Satellite data	Location	Ecological	Model Statistics		Reference
					R ²	RMSE (Mgha)	
1	Random Forest	Sentinel -2	Yok Don National Park, Vietnam	Evergreen and deciduous broadleaved fores	0.81	36.67	(Dang et al., 2019)
2		Sentinel -2	Parsa National Park, Nepal	Central-Southern part of Nepal,	0.81	25.57	(Pandit, Tsuyuki, & Dube, 2018)
3		Sentinel -2	Rhodopes mountain range, Greece	Mediterranean forest	0.63	63.11	(Chrysafis, Mallinis, Siachalou, & Patias, 2017)
4		Sentinel -2	Doi Inthanon Nation Park, Chiangmai, Thailand	Deciduous forest	0.98	6.04	This study
5		ICESat/GLAS and WorldView2	Uttarakhand, India	Tropical Moist Deciduous forest, subtropical climate	0.84	20.57	(Dhanda et al., 2017)
6		Landsat 7 ETM+	Zhejiang Province, China	Subtropical monsoon climate	0.63	26.22	(Wu et al., 2016)
7	Support Vector Regression (SVR)	Landsat 7 ETM+	Zhejiang Province, China	Subtropical monsoon climate	0.38	34.61	(Wu et al., 2016)
8		ICESat/GLAS and WorldView2	Uttarakhand, India		0.89	13.60	(Dhanda et al., 2017)

5. CONCLUSION AND FUTURE WORK

In this study, Sentinel-2 was used to generate the burn map in Doi Inthanon national park in northern Thailand. Sentinel-2 satellite images were downloaded before fire event and after fire event. Both the Sentinel datasets Satellite images were calculated by the burn index for assessing fire-damaged areas and compared burn mapping of GISTDA based on Landsat 8 satellite image and checked number of active fire hotspots.

The result shows that RBR is the best performance for assessing of burn area in this study. The RBR index results generally showed similar trends with reference data and the accuracy is higher than BAIS2 and dNBR indices.

Therefore, Sentinel-2 satellite images are useful in evaluating burned areas or the areas that are damaged by fire. These satellite images can also monitor the fires faster than Landsat satellite image due to having a high spatial resolution (10m,20m) and a short temporal resolution. Furthermore, This study shows that applying new techniques and methods in remote sensing could improve the accuracy in analyzing the information.

Random Forest (RF) and Support Vector Machine (SVM) in machine-learning model were used to improve the accuracy of satellite image analysis with a more complex algorithm. In this section, the burned area of the RBR index is used to assess the loss of above-ground biomass, and the result found that most of the burned areas are the deciduous forests. The Vegetation indices (Vis) combine and forest inventory parameters were used to estimate above-ground biomass loss in damage area from forest fires and compare the accuracy of the biomass model using Machine Learning method (RF, SVM). 47 sample plots and 5 vegetation indice were considered to calculate the loss of aboveground biomass. The 6-fold cross-validation was used to evaluate model effectiveness.

The results of these analyses showed that the RF model is the lowest root mean square error from predicted and observed $AGB(W_s+W_l+W_b)$, $AGB(W_l)$ and highest coefficient of determination. The RF model was the most accurate model for estimating AGB in this study area. These results demonstrated that Sentinel-2 satellite

is a source of valuable information for the monitor after the fire event. It is also suitable for assessing the changes in vegetation, forestry, agriculture and other areas.

In summary, the results of the research can be used as a guideline in planning to prevent the damage and sustainable forest management. For future research, to improve the assessment of aboveground biomass and assess the damage of forest fires, LiDAR data, high-resolution satellite and aerial imagery from drone should be used for the evaluation, combining with optical satellite data and field forest inventory.

This study examines the application of remote sensing with machine learning concepts which is considered to be suitable for evaluating biomass. The limitation of this study is the data collecting process in the field. Due to the time constraint, the data in the sample plot cannot be fully collected, for example, the collection of the sapling, seeding that these data have an effect on the estimation of biomass and affect by forest fires. Therefore, it is necessary to improve the study for future research as to reduce errors in the evaluation of biomass and assess damaged areas from fire.

In the future research, the methods of this study should be used for analysis in other areas as a basis for comparison of data accuracy, variables obtained from satellites. Therefore, future research should be conducted to extract the information forest changes with deep learning methods or neural network and monitoring the forest change with time-serials remote sensing data and evaluating the impact of these data changes on the regional environment.

REFERENCES

- Alpaydin, E. (2014). *Introduction to Machine Learning*: The MIT Press.
- Askar, Nuthammachot, N., Phairuang, W., Wicaksono, P., & Sayektiningsih, T. (2018). Estimating Aboveground Biomass on Private Forest Using Sentinel-2 Imagery. *Journal of Sensors*, 2018, 1-11. doi:10.1155/2018/6745629
- Banko, G. (1998). A Review of Assessing the Accuracy of Classifications of Remotely Sensed Data and of Methods Including Remote Sensing Data in Forest Inventory.
- Bishop, C. M. (2006). *Pattern Recognition and Machine Learning* (second ed.). University of California, Berkeley: Springer.
- Botchkarev, A. (2018). Performance Metrics (Error Measures) in Machine Learning Regression, Forecasting and Prognostics: Properties and Typology.
- Cansler, C. A. (2011). *Drivers of burn severity in the northern Cascade Range, Washington, USA* (Master of Science Thesis), University of Washington USA
- Cao, L., Pan, J., Li, R., Li, J., & Li, Z. (2018). Integrating Airborne LiDAR and Optical Data to Estimate Forest Aboveground Biomass in Arid and Semi-Arid Regions of China. *Remote Sensing*, 10(4). doi:10.3390/rs10040532
- Cao, Q., Miao, Y., Shen, J., Yu, W., Yuan, F., Cheng, S., . . . Liu, F. (2016). Improving in-season estimation of rice yield potential and responsiveness to topdressing nitrogen application with Crop Circle active crop canopy sensor. *Precision Agriculture*, 17(2), 136-154. doi:10.1007/s11119-015-9412-y
- Chen, J.-C., Yang, C. M., Wu, S.-T., Chung, Y. L., Charles, A. L., & Chen, C.-T. (2007). Leaf chlorophyll content and surface spectral reflectance of tree species along a terrain gradient in Taiwan's Kenting National Park. 48, 71-77.
- Chen, L., Ren, C., Zhang, B., Wang, Z., & Xi, Y. (2018). Estimation of Forest Aboveground Biomass by Geographically Weighted Regression and Machine Learning with Sentinel Imagery. *Forests*, 9(10). doi:10.3390/f9100582
- Chrysafis, I., Mallinis, G., Siachalou, S., & Patias, P. (2017). Assessing the relationships between growing stock volume and Sentinel-2 imagery in a Mediterranean forest ecosystem. *Remote Sensing Letters*, 8(6), 508-517. doi:10.1080/2150704X.2017.1295479

- Congalton, R. G., & Green, K. (1998). *Assessing the Accuracy of Remotely Sensed Data : Principles and Practices*. New York: Lewis Publishers.
- CURRAN, P. J., DUNGAN, J. L., & GHGLZ3, H. L. (1990). Exploring the relationship between reflectance red edge and chlorophyll content in slash pine. *Tree Physiology* 7, 33-48.
- Dang, A. T. N., Nandy, S., Srinet, R., Luong, N. V., Ghosh, S., & Senthil Kumar, A. (2019). Forest aboveground biomass estimation using machine learning regression algorithm in Yok Don National Park, Vietnam. *Ecological Informatics*, 50, 24-32. doi:10.1016/j.ecoinf.2018.12.010
- Delegido, J., Verrelst, J., Alonso, L., & Moreno, J. (2011). Evaluation of Sentinel-2 red-edge bands for empirical estimation of green LAI and chlorophyll content. *Sensors (Basel)*, 11(7), 7063-7081. doi:10.3390/s110707063
- Dhanda, P., Nandy, S., Kushwaha, S. P. S., Ghosh, S., Murthy, Y. V. N. K., & Dadhwal, V. K. (2017). Optimizing spaceborne LiDAR and very high resolution optical sensor parameters for biomass estimation at ICESat/GLAS footprint level using regression algorithms. *Progress in Physical Geography: Earth and Environment*, 41(3), 247-267. doi:10.1177/0309133317693443
- DNP. (2007). *Plants of Doi inthanon Nation Park* (1 ed.). Bangkok: Herbarium office, Bangkok.
- DNP. (2019). *The statistics of forest fire occurrences in Thailand from 1998-2019*. Retrieved from http://www.dnp.go.th/ForestFire/web/frame/statistic_all.html:
- EROS (Producer). (2019, November 20). USGS EROS Archive - Sentinel-2 - Comparison of Sentinel-2 and Landsat. <https://www.usgs.gov>. Retrieved from https://www.usgs.gov/centers/eros/science/usgs-eros-archive-sentinel-2-comparison-sentinel-2-and-landsat?qt-science_center_objects=0#qt-science_center_objects
- ESA. (2015). *Sentinel-2 User Handbook*. Retrieved from https://sentinel.esa.int/documents/247904/685211/Sentinel-2_User_Handbook:
- Escuin, S., Navarro, R., & Fernández, P. (2008). Fire severity assessment by using NBR (Normalized Burn Ratio) and NDVI (Normalized Difference Vegetation Index)

- derived from LANDSAT TM/ETM images. *International Journal of Remote Sensing*, 29(4), 1053-1073. doi:10.1080/01431160701281072
- Filipponi, F. (2018). BAIS2: Burned Area Index for Sentinel-2. *Proceedings*, 2(7). doi:10.3390/ecrs-2-05177
- Filipponi, F. (2019). Exploitation of Sentinel-2 Time Series to Map Burned Areas at the National Level: A Case Study on the 2017 Italy Wildfires. *Remote Sensing*, 11(6). doi:10.3390/rs11060622
- FIRMS. (2019). *Active Fire Data*. Retrieved from https://firms.modaps.eosdis.nasa.gov/active_fire/#firms-shapefile:
- GISTDA. (2019). *Summary of forest fires and smog situations with satellite images*. Retrieved from <http://fire.gistda.or.th/>:
- Gitelson, A. A., Kaufman, Y. J., & Merzlyak, M. N. (1996). Use of a green channel in remote sensing of global vegetation from EOS-MODIS. *Remote Sensing of Environment*, 58(3), 289-298. doi:[https://doi.org/10.1016/S0034-4257\(96\)00072-7](https://doi.org/10.1016/S0034-4257(96)00072-7)
- IPCC. (2006). *IPCC Guidelines for National Greenhouse Gas Inventories*. In *International Panel on Climate Change*.
- Key, C. H., & Benson, N. C. (2006). *Landscape Assessment: Ground measure of severity, the Composite Burn Index; and Remote sensing of severity, the Normalized Burn Ratio* (RMRS-GTR-164-CD: LA 1-51). Retrieved from Ogden, UT: <http://pubs.er.usgs.gov/publication/2002085>
- Kohavi, R., & Provost, F. (1998). Glossary of Terms. *Machine Learning*, 2, 271-274. doi:10.1023/A:1017181826899
- Malenovský, Z., Rott, H., Cihlar, J., Schaepman, M. E., García-Santos, G., Fernandes, R., & Berger, M. (2012). Sentinels for science: Potential of Sentinel-1, -2, and -3 missions for scientific observations of ocean, cryosphere, and land. *Remote Sensing of Environment*, 120, 91-101. doi:<https://doi.org/10.1016/j.rse.2011.09.026>
- Mallinis, G., Mitsopoulos, I., & Chrysafi, I. (2017). Evaluating and comparing Sentinel 2A and Landsat-8 Operational Land Imager (OLI) spectral indices for estimating fire severity in a Mediterranean pine ecosystem of Greece.

GIScience & Remote Sensing, 55(1), 1-18.

doi:10.1080/15481603.2017.1354803

- Marino, E., Guillen-Climent, M., Ranz Vega, P., & Tomé, J. (2016). Fire severity mapping in Garajonay National Park: comparison between spectral indices. *FLAMMA*, 7, 22-28.
- McFeeters, S. K. (2007). The use of the Normalized Difference Water Index (NDWI) in the delineation of open water features. *International Journal of Remote Sensing*, 17(7), 1425-1432. doi:10.1080/01431169608948714
- Miller, P., Stolte, K., Duriscoe, D., & Pronos, J. (1996). Evaluating ozone air pollution effects on pines in the western United States. Forest Service general technical report.
- Muukkonen, P. (2007). Generalized allometric volume and biomass equations for some tree species in Europe. *European Journal of Forest Research*, 126(2), 157-166. doi:10.1007/s10342-007-0168-4
- Navarro, G., Caballero, I., Silva, G., Parra, P.-C., Vázquez, Á., & Caldeira, R. (2017). Evaluation of forest fire on Madeira Island using Sentinel-2A MSI imagery. *International Journal of Applied Earth Observation and Geoinformation*, 58, 97-106. doi:10.1016/j.jag.2017.02.003
- Ogawa, H. (1965). Comparative ecological studies on three main types of forest vegetation in Thailand. II. Plant biomass. *Nature and Life in Southeast Asia*, 4, 49-80.
- Oladipupo, T. (2010). Types of Machine Learning Algorithms. In *New Advances in Machine Learning*.
- Padmapriya, S. (2015). A Study on Algorithmic Approaches and Mining Methodologies In Data Mining. *International Journal of Computer Science Trends and Technology (IJCST)*, 3(1), 106-109.
- Pandit, S., Tsuyuki, S., & Dube, T. (2018). Estimating Above-Ground Biomass in Sub-Tropical Buffer Zone Community Forests, Nepal, Using Sentinel 2 Data. *Remote Sensing*, 10(4). doi:10.3390/rs10040601

- Parks, S., Dillon, G., & Miller, C. (2014). A New Metric for Quantifying Burn Severity: The Relativized Burn Ratio. *Remote Sensing*, 6(3), 1827-1844.
doi:10.3390/rs6031827
- RFD. (2018). *Final Report Forest Classification Project 2017-2018*. Retrieved from <https://www.forest.go.th/land/wp-content/uploads/sites/29/2019/03/final-report-2561.pdf>:
- Rouse, J. W., Jr., Haas, R. H., Schell, J. A., & Deering, D. W. (1974). *Monitoring vegetation systems in the Great Plains with ERTS*. Paper presented at the "NASA. Goddard Space Flight Center 3d ERTS-1 Symp., Vol. 1, Sect. A", United States. Conference Paper retrieved from <https://ntrs.nasa.gov/search.jsp?R=19740022614>
- Suresh Babu, K. V., Roy, A., & Aggarwal, R. (2018). Mapping of Forest Fire Burned Severity Using the Sentinel Datasets. *ISPRS - International Archives of the Photogrammetry, Remote Sensing and Spatial Information Sciences*, XLII-5, 469-474. doi:10.5194/isprs-archives-XLII-5-469-2018
- TGO. (2011). *A guidebook for the potential of plant species for encouragement under the Clean Development Mechanism Project in the Forest Section* Retrieved from http://www.tgo.or.th/2015/thai/download_cat.php?cid=2:
- Wu, C., Shen, H., Shen, A., Deng, J., Gan, M., Zhu, J., . . . Wang, K. (2016). Comparison of machine-learning methods for above-ground biomass estimation based on Landsat imagery. *Journal of Applied Remote Sensing*, 10(3). doi:10.1117/1.Jrs.10.035010
- Xiao, C. (2015). *Using Machine Learning for Exploratory Data Analysis and Predictive Models on Large Datasets*. (MASTER'S THESIS), Stavanger, Retrieved from <https://core.ac.uk/download/pdf/52118152.pdf>



APPENDIX

1. Appendix A Tree species list

The Tree specific name online in the following website :

<http://t-fern.forest.ku.ac.th/Forest/index.php>

Table A. Tree species list

No.	Tree Species	Family
1	<i>Adenanthera pavonina</i> Linn.	MIMOSACEAE
2	<i>Albizia odoratissima</i> Benth.	MIMOSACEAE
3	<i>Alstonia scholaris</i> R. Br.	APOCYNACEAE
4	<i>Anthocephalus chinensis</i> Rich. ex Walp.	RUBIACEAE
5	<i>Antidesma ghaesembilla</i> Gaertn.	STILAGINACEAE
6	<i>Antidesma sootepense</i> Craib	STILAGINACEAE
7	<i>Aporosa villosa</i> Baill.	EUPHORBIACEAE
8	<i>Bombax valetonii</i> Hichr.	BOMBACACEAE
9	<i>Buchanania latifolia</i> Roxb.	ANACARDIACEAE
10	<i>Canarium subulatum</i> Guill.	BURSERACEAE
11	<i>Chukrasia velutina</i> Wight & Arn.	MELIACEAE
12	<i>Cratoxylum cochinchinense</i> Blume	GUTTIFERAE
13	<i>Dalbergia oliveri</i> Gamble ex Prain	PAPILIONOIDEAE
14	<i>Dipterocarpus tuberculatus</i> Roxb.	DIPTEROCARPACEAE
15	<i>Elaeocarpus hygrophilus</i> Kurz	ELAEOCARPACEAE
16	<i>Eugenia cumini</i> Druce	MYRTACEAE
17	<i>Flacourtia indica</i> Merr.	FLACOURTIACEAE
18	<i>Gardenia oftusfolia</i> Roxb.	RUBIACEAE
19	<i>Gardenia sootepensis</i> Hutch.	RUBIACEAE
20	<i>Gomphia serrata</i> Kanis	OCHNACEAE
21	<i>Grewia eriocarpa</i> Juss.	TILIACEAE
22	<i>Ixora cibdela</i> Craib	RUBIACEAE
23	<i>Kydia calycina</i> Roxb.	MALVACEAE

Table A. Tree species list

No.	Tree Species	Family
24	<i>Lagerstroemia duperreana</i> Pierre	LYTHRACEAE
25	<i>Lagerstroemia macrocarpa</i> Wall	LYTHRACEAE
26	<i>Lannea coromandelica</i> Merr.	ANACARDIACEAE
27	<i>Markhamia stipulata</i> Seem.	BIGNONIACEAE
28	<i>Melanorrhoea usitata</i> Wall.	ANACARDIACEAE
29	<i>Memecylon scutellatum</i> Naud.	MEMECYLACEAE
30	<i>Millettia brandisiana</i> Kurz	PAPILIONACEAE
31	<i>Mitragyna rotundifolia</i> Ktze.	RUBIACEAE
32	<i>Moghania sootepensis</i> Li	PAPILIONACEAE
33	<i>Morinda coreia</i> Ham.	RUBIACEAE
34	<i>Morinda elliptica</i> (Hook.f.) Ridl.	MELASTOMATACEAE
35	<i>Paranephelium longifoliolatum</i> Lec.	SAPINDACEAE
36	<i>Phyllanthus emblica</i> Linn.	EUPHORBIACEAE
37	<i>Pinus merkusii</i> Jungh. & de Vriese	PINACEAE
38	<i>Pterocarpus macrocarpus</i> Kurz	PAPILIONACEAE
39	<i>Quercus kerrii</i> Craib	FAGACEAE
40	<i>Randia dasycarpa</i> Bakh. f.	RUBIACEAE
41	<i>ratoxylum formosum</i> (Jack.) Dyer subsp. <i>Pruniflorum</i> Gogel.	CLUSIACEAE (GUTTIFERAE)
42	<i>Schleichera oleosa</i> Merr.	SAPINDACEAE
43	<i>Shorea obtusa</i> Wall.	DIPTEROCARPACEAE
44	<i>Shorea siamensis</i> Miq.	DIPTEROCARPACEAE
45	<i>Sindora siamensis</i> Teijsm. ex Miq.	CAESALPINIACEAE
46	<i>Stereospermum neuranthum</i> Kurz	BIGNONIACEAE
47	<i>Spondias bipinnata</i> Airy Shaw & Forman	ANACARDIACEAE
48	<i>Terminalia alata</i> Heyne ex Roth	COMBRETACEAE
49	<i>Terminalia chebula</i> Retz.	COMBRETACEAE
50	<i>Terminalia corticosa</i> Pierre ex Laness.	COMBRETACEAE

Table A. Tree species list

No.	Tree Species	Family
51	<i>Vitex pinnata</i> Linn.	VERBENACEAE
52	<i>Wendlandia paniculata</i> A. DC.	RUBIACEAE
53	<i>Wendlandia tinctoria</i> A. DC.	RUBIACEAE
54	<i>Xylia xylocarpa</i> (Roxb.) Jaub. <i>Var. kerrii</i> (Craib & Hutch.) Nielsen	MIMOSACEAE

2. Appendix B

List of publications and papers presented

2.1 Zhenfeng Shao, Penghao Tang, Zhongyuan Wang, Nayyer Saleem, Sarath Yam and Chatpong Sommai, BRRNet : A Fully Convolutional Neural Network for Automatic Building Extraction From High-Resolution Remote Sensing Images. *Remote Sens.* 2020, 12, 1050 ; doi :10.3390/rs12061050.

2.2 Zhenfeng Shao, Xiaoyi Long, Bowen Cai, Sarath Yam, Chatpong Sommai. Extraction of Urban Impervious Surface Based on High Resolution Remote Sensing Images. CPGIS international conference. 2020, (Published)

2.3 Chatpong Sommai, Zhenfeng Shao. Forest fire Damage Assessment using Sentinel-2 Satellite Imagery in Doi Inthanon National Park in Chiangmai Province, Thailand. 2020 Sirindhorn Conference on Geo-Informatics, 2020. (submitted)

2.4 Zhenfeng Shao, Chatpong Sommai, Ya Zhang. Forest fire Damage Assessment Model using Multi-source remote sensing image, *IEEE Journal of Selected Topics in Applied Earth Observations and Remote Sensing*, 2020. (submitted)

BIOGRAPHY

NAME Chatpong Sommai

DATE OF BIRTH 15 August 1988

PLACE OF BIRTH Thailand

PRESENT ADDRESS 56/301 Ladsawai sub-district, Lamlukka district,
Pathumthani, Thailand

POSITION HELD Forestry Technical Officer, Practitioner level

EDUCATION B.Sc. (Forestry) with Second Class Honors, Forest
Resource Management (Forest Management Option),
Kasetsart University, Bangkok, THAILAND

